

ATLAS実験の最近の物理結果から

佐藤構二

宇宙史センター 構成員会議

2019年11月18日(月)

LHC実験

スイス・アルプス山脈

世界最高エネルギーでの加速器実験

$\sqrt{s} \leq 14 \text{ TeV}$ での陽子・陽子衝突

2010年 LHC加速器稼動開始。

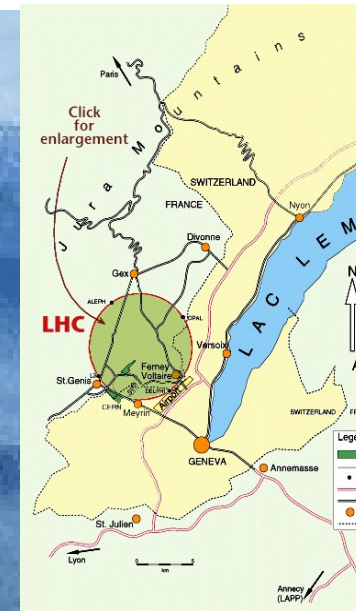
2011-12年 物理Run開始。Ecm=7 – 8 TeV, 25 fb⁻¹のデータ取得。

2012年 LHC加速器のATLAS/CMS両実験がヒッグス粒子を発見。

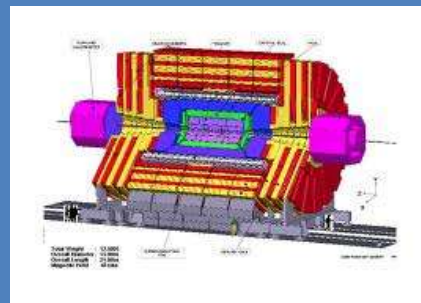
2015-18年 エネルギーをEcm=13 TeVに上げてRun 2実験。

2021-2023年 Run 3。Ecm=14 TeV, ~300 fb⁻¹のデータセット

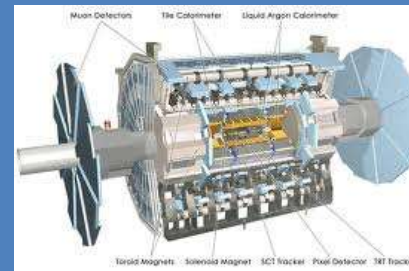
2026-203X年 HL-LHC実験。~3000 fb⁻¹の大データセット。



CMS実験



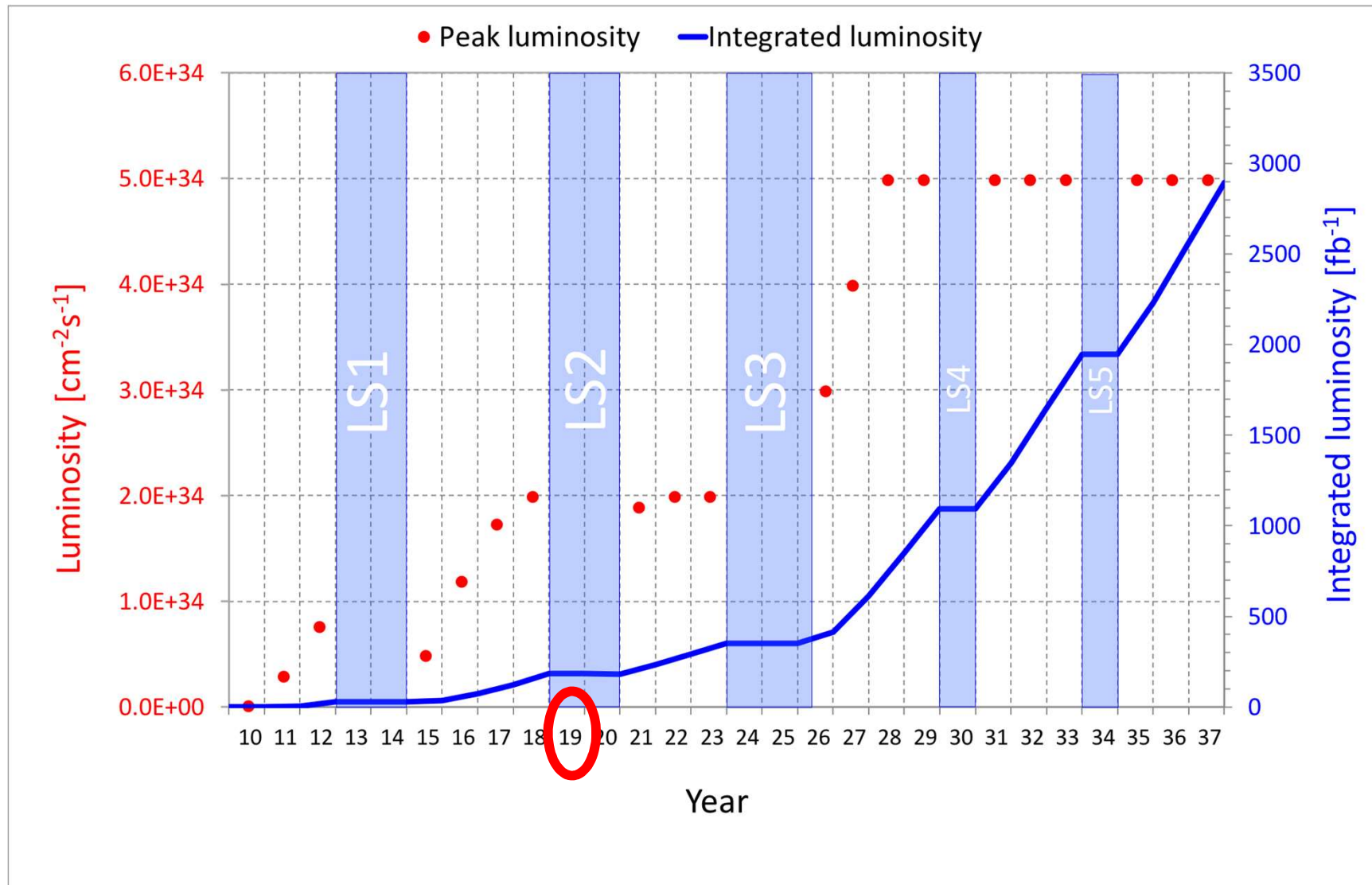
ATLAS実験



円周27km

陽子を最大7 TeVまで加速して正面衝突

LHCの長期将来計画



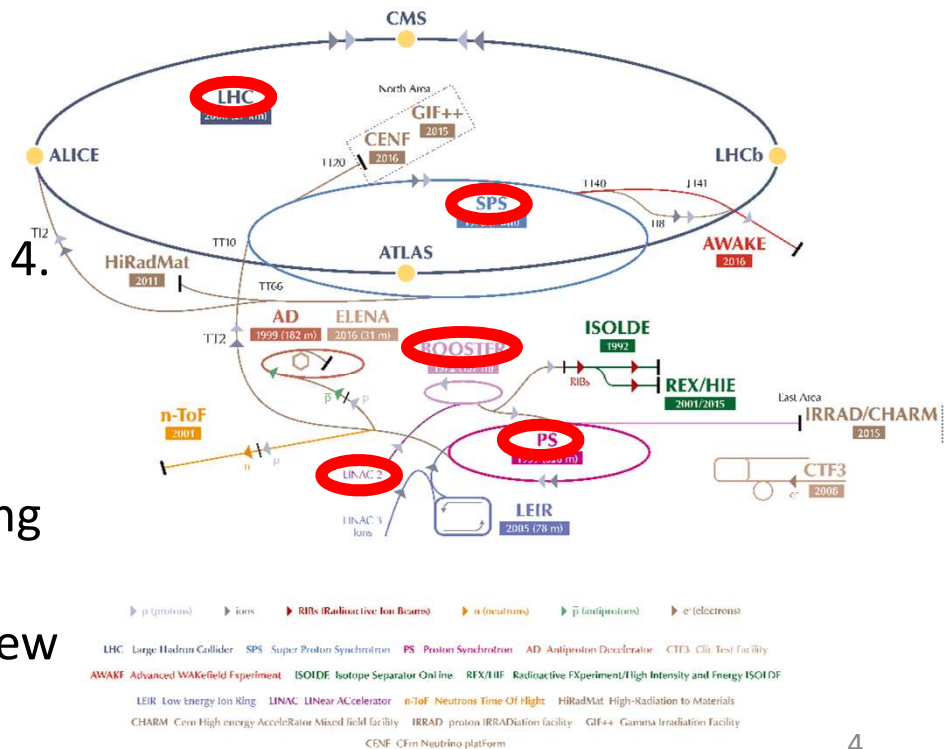
Accelerator LS2 Upgrades

- 2019-2020: Long Shutdown (LS2) preparing for Run 3 in 2021-2023.

Key Plans for LS2 Accelerator Upgrades

<https://home.cern/news/news/accelerators/key-plans-next-two-years-lhc>

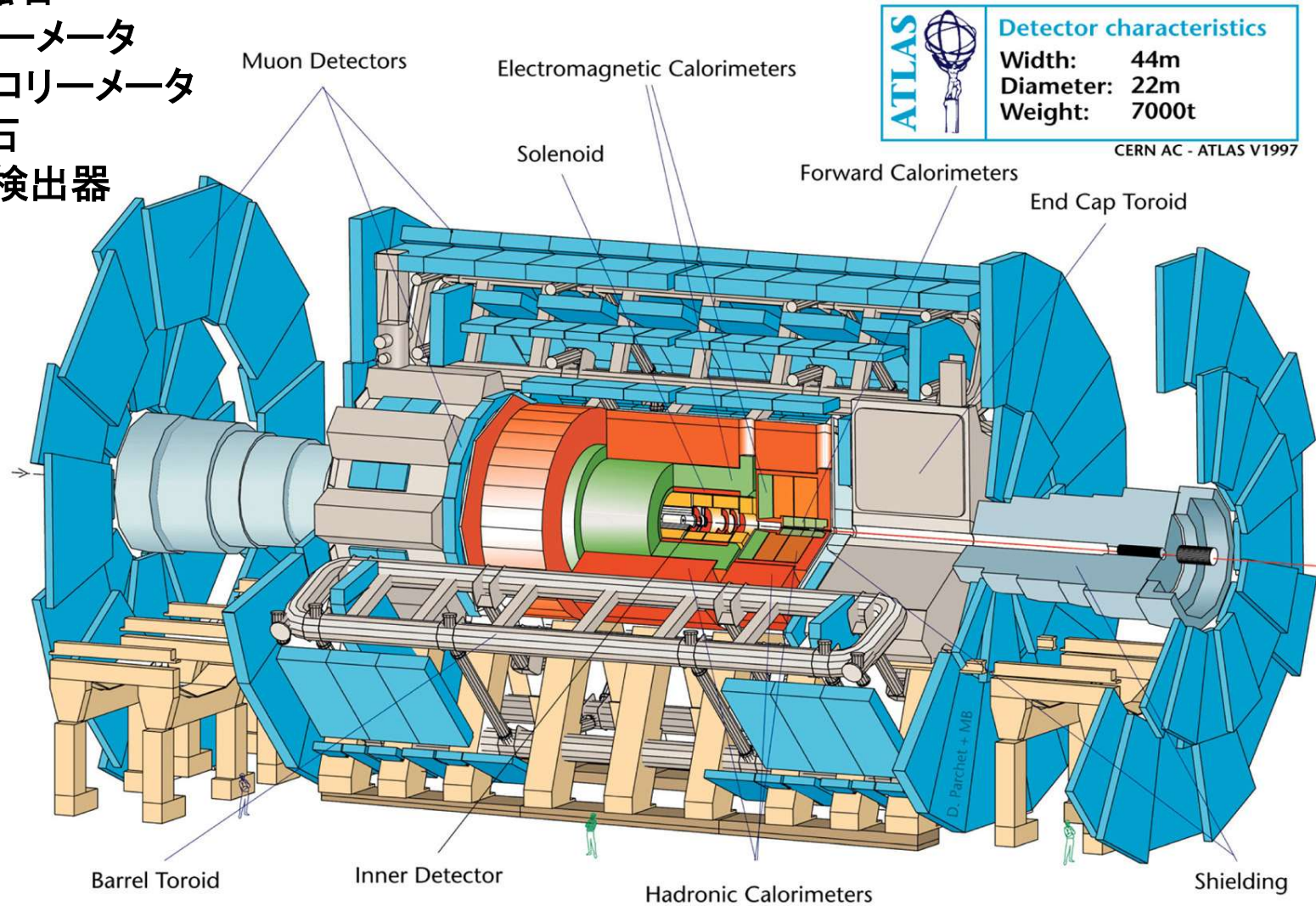
- Preparation for HL-LHC, as well as Run 3 and maintenance.
- More intense, concentrated beam, with new Linac accelerating H- instead of proton.
 - Replace Linac 2 with new Linac 4.
 - Upgrade Booster injection.
 - New RF system in SPS.
- Bring beam energy up to 7 TeV.
 - Consolidate the diodes providing current to dipole magnets
- ~20 magnet replacements, install new lifts, ...



ATLAS検出器

総重量 7,000 t

- シリコン検出器
- 飛跡検出器
- ソレノイド磁石
- 電磁カロリメータ
- ハドロンカロリメータ
- トロイド磁石
- ミューオン検出器

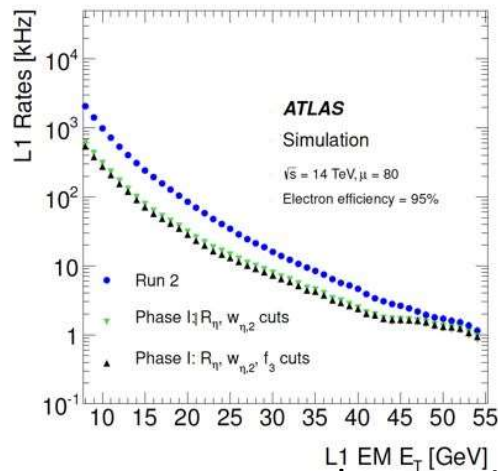
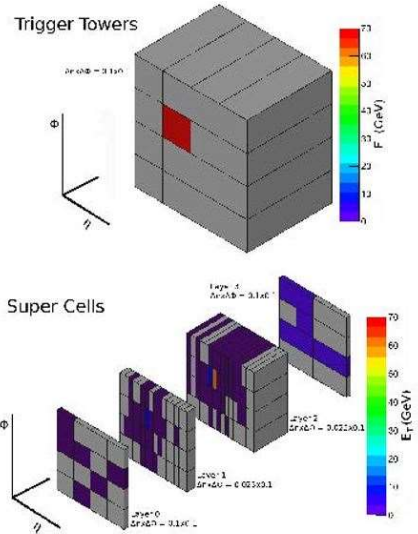


- 最高エネルギーでの、**さまざまな素粒子反応の研究**
 - ヒッグス粒子、標準理論、トップクォーク、Bメソン、超対称性、新物理探索、重イオン衝突...

ATLAS LS2 Upgrades

L1 Calo Trigger Upgrade

読み出しを細分化することで、他バ
ンチのヒットの影響を減らす。

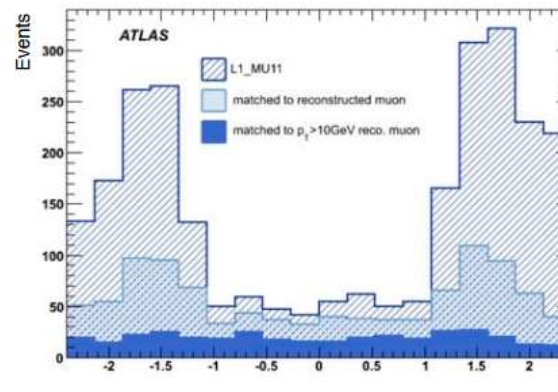
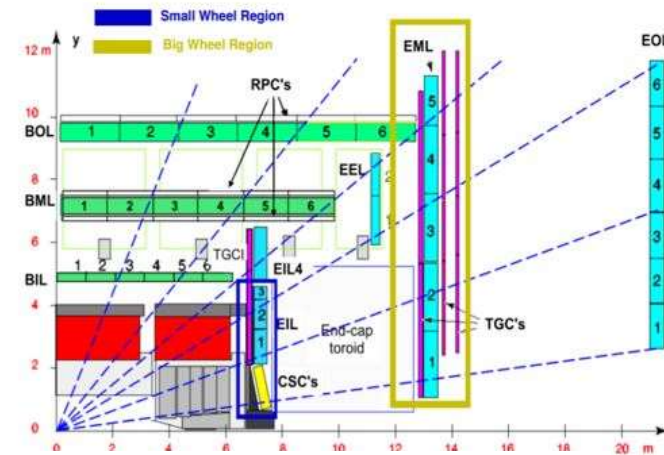


Improvement on Jet and MET triggers, too.

Nucl.Instrum.Meth. A824 (2016) 374-378

New Muon Small Wheel For L1 Trigger

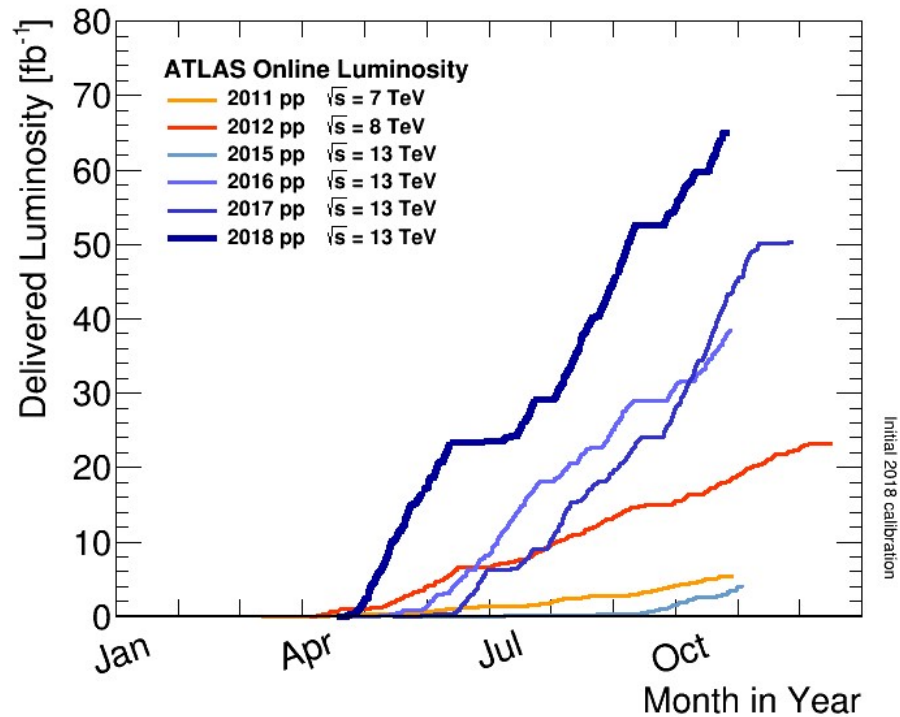
内層に新しいトリガーチェンバーを入れる。



arXiv:1810.01394

FTK Upgrade – new track trigger in L2 trigger.
TDAQ Upgrade

Luminosities in Run 2



Run 1	E_{CM} (TeV)	integ lumi [fb^{-1}]
2011	7	5
2012	8	21

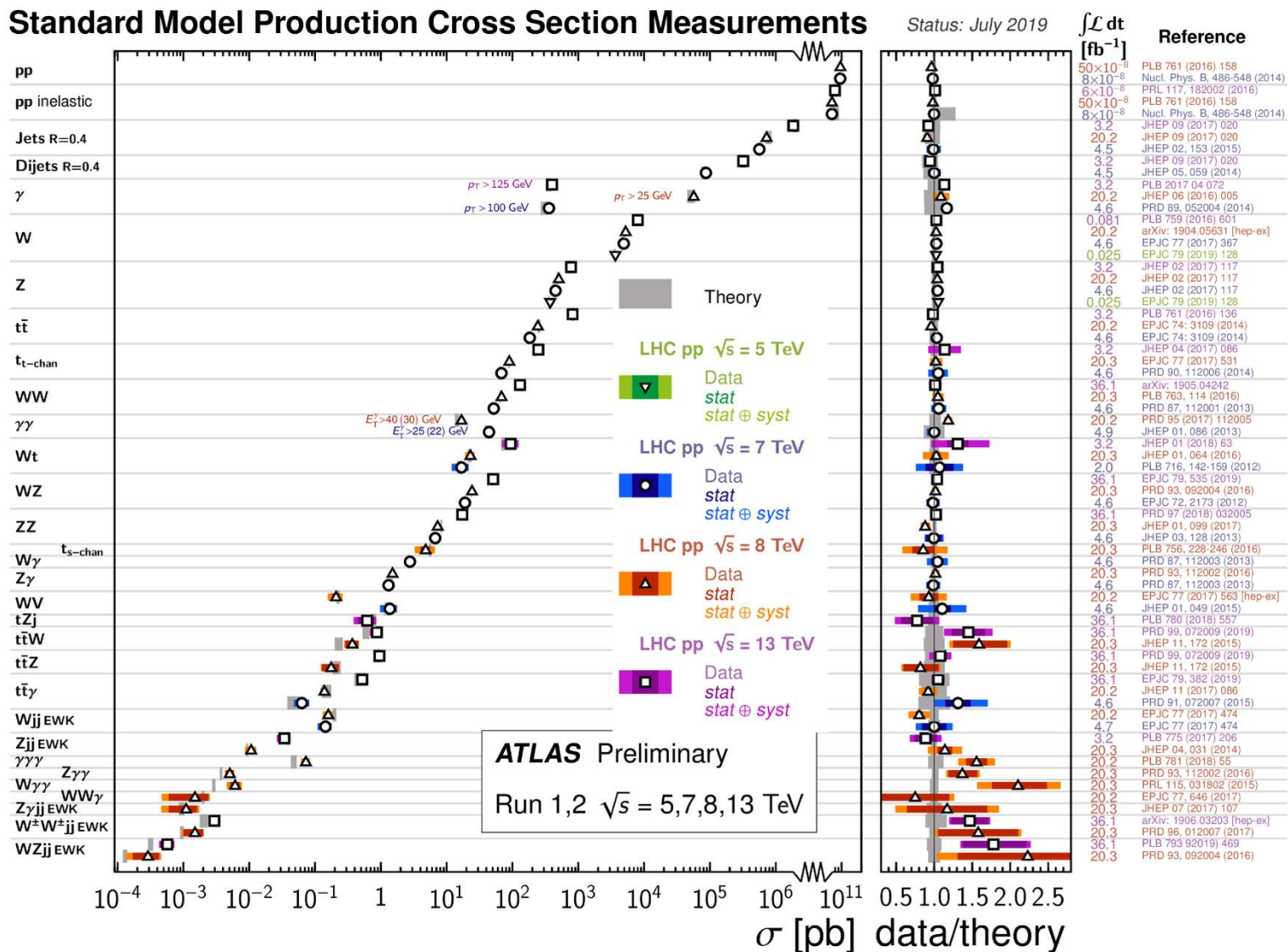
$E_{CM} = 13$ (TeV)

Run 2	Peak lumi $E_{34} \text{ cm}^{-2}\text{s}^{-1}$	Days pp physics	Recorded integ lumi [fb^{-1}]	Good for Physics [fb^{-1}] 累積
2015	0.5	56	3.9	3.2
2016	1.4	122	36.0	36
2017	1.9	150	46.9	80
2018	2.1	152	65.0	139

標準理論の大成功

Standard Model Production Cross Section Measurements

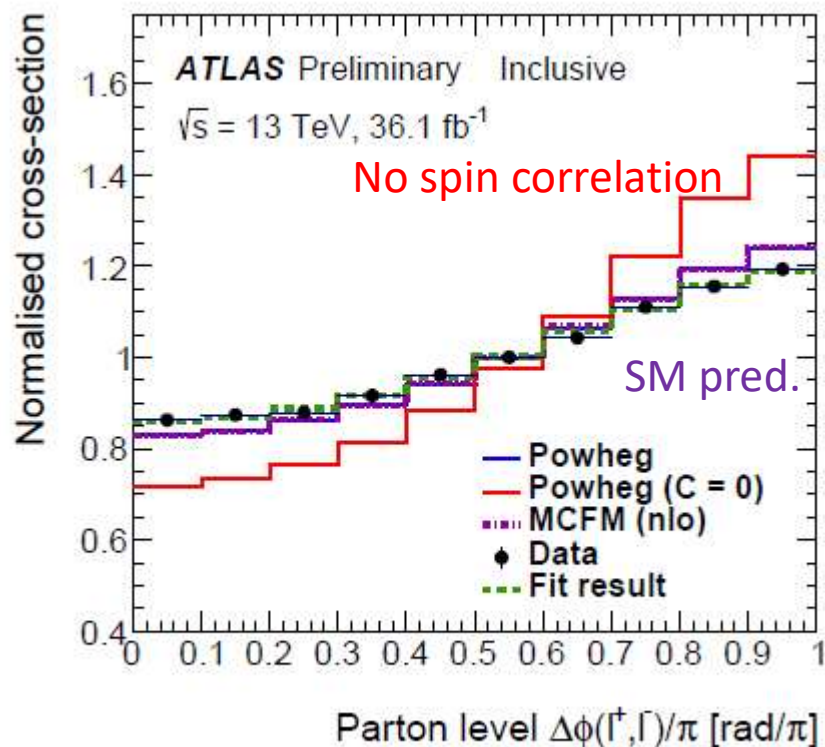
Status: July 2019



15桁にわたって、理論=実験がよく合っている。

Top Spin Correlation

2018年11月
宇宙市センター構成員会議



- $t\bar{t} \rightarrow (Wb)(Wb) \rightarrow (e\nu b)(\mu\nu b)$
- e と μ の間の角度相関。
- SM(NLO QCD)の予言値よりも強い相関がみられた。
- テンプレート・フィット

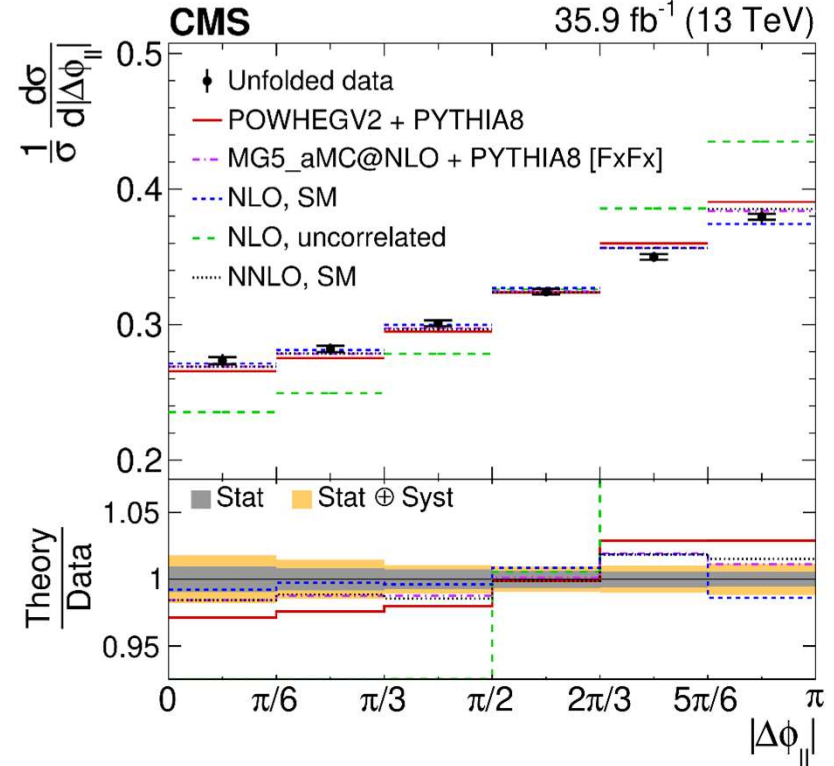
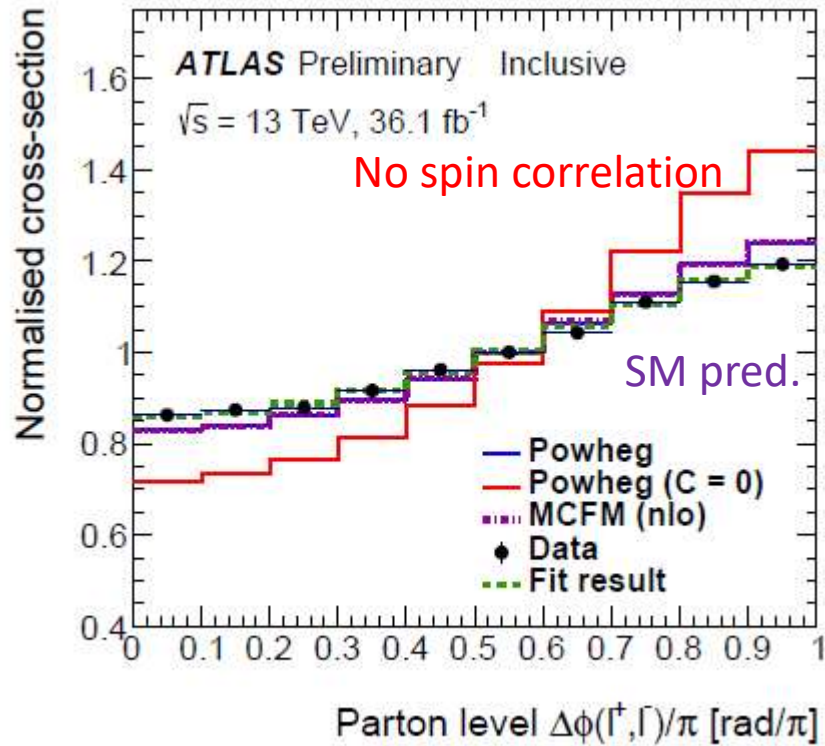
$$n_i = f_{SM} \cdot n_{spin} + (1 - f_{SM}) \cdot n_{nospin}$$
 フィット結果:

$$f_{SM} = 1.250 \pm 0.026 \pm 0.063$$
- SMからのずれ: 3.2σ (syst込み)

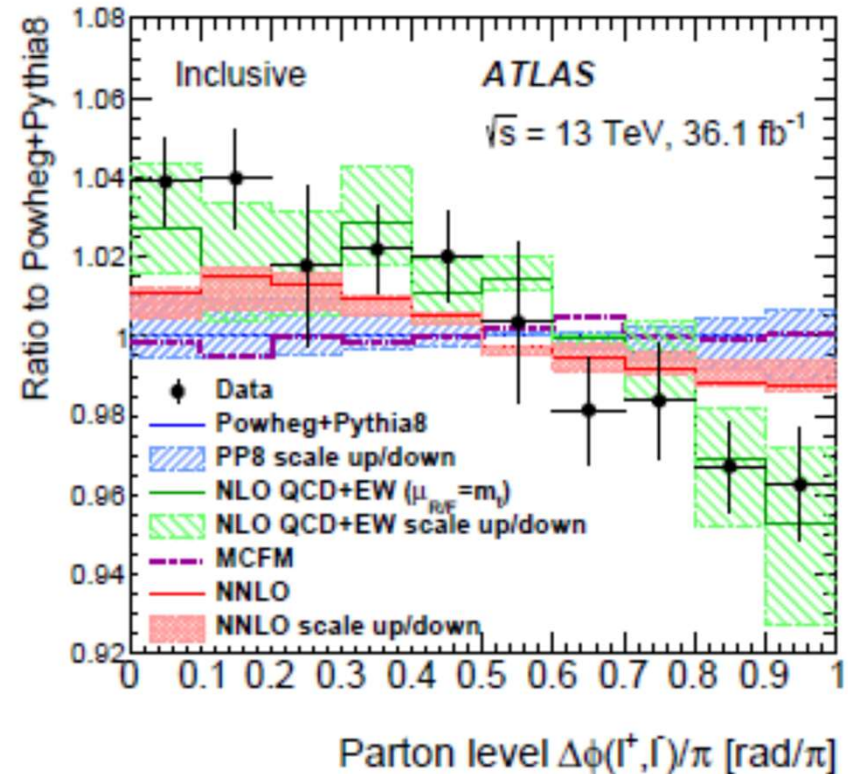
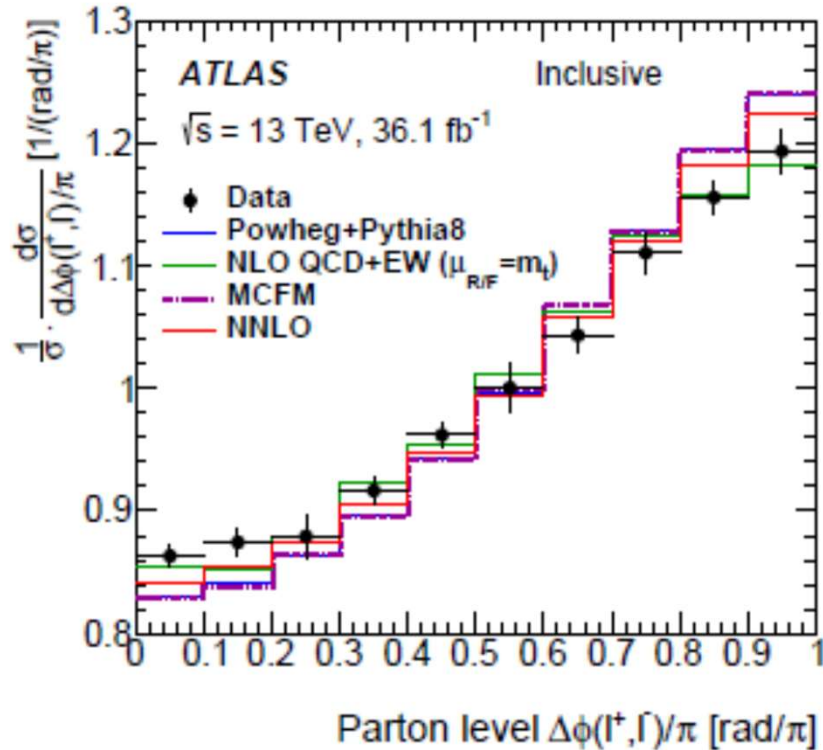
Top Spin Correlation CMSの分布

arXiv:1907.03729

35.9 fb⁻¹ (13 TeV)

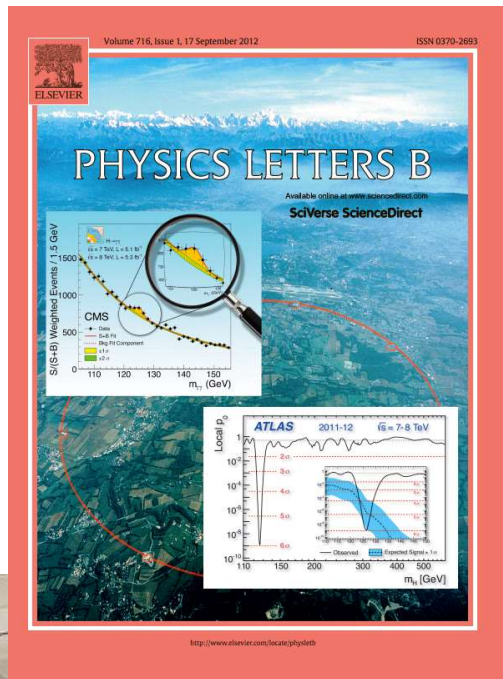


Top Spin Correlation 今年の夏のアップデート



- NLO QCD+EWKはデータをよく再現する。
- 理論計算の精度が足りていないせいと結論できるか。

ヒッグス粒子発見の発表



2012年7月4日 LHC加速器の
ATLAS/CMS両実験が発見を報告

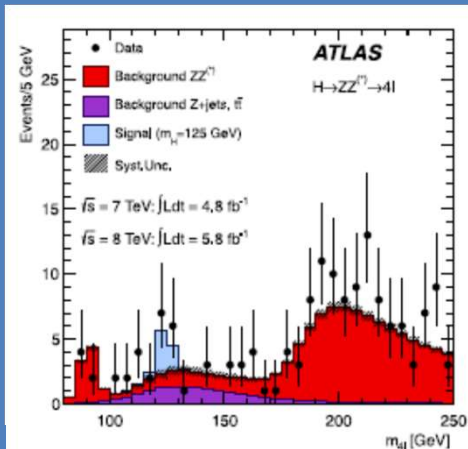
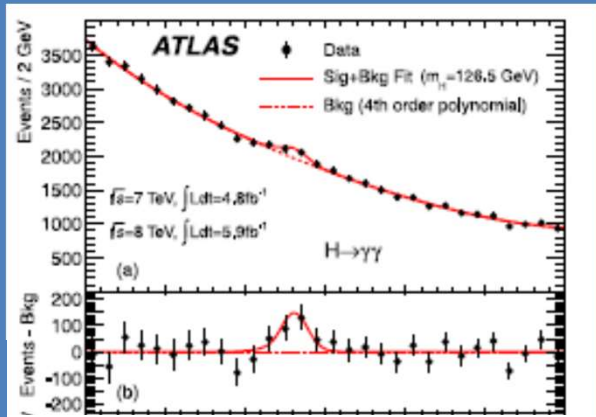
2013年 アングラール、ヒッグス
がノーベル物理学賞を受賞



ヒッグス発見チャンネルの現在

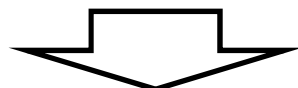
2012年夏、ヒッグス粒子発見時のデータ

[Phys. Lett. B 716 \(2012\) 1-29](#)

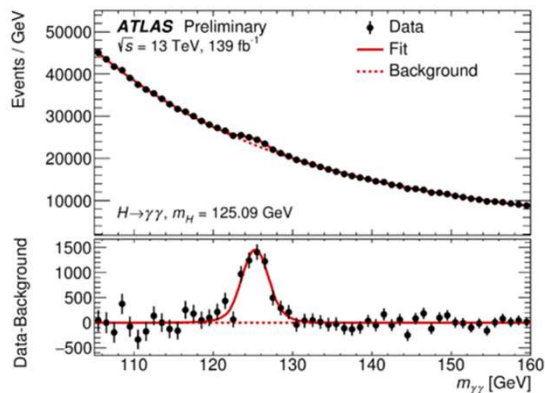


2チャンネル合わせて5.9 σ .

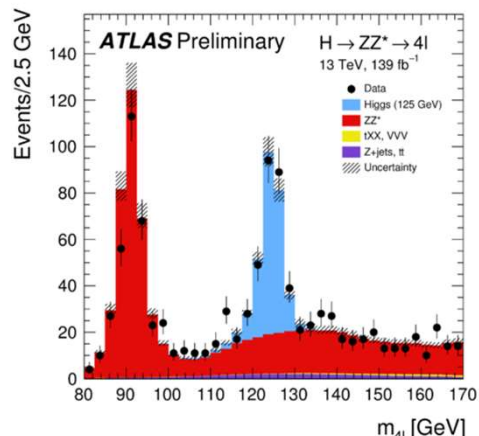
$H \rightarrow \gamma\gamma$



$H \rightarrow ZZ^* \rightarrow 4l$



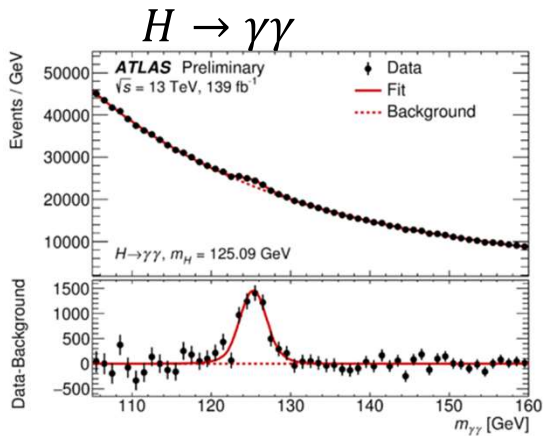
ATLAS-CONF-2019-032



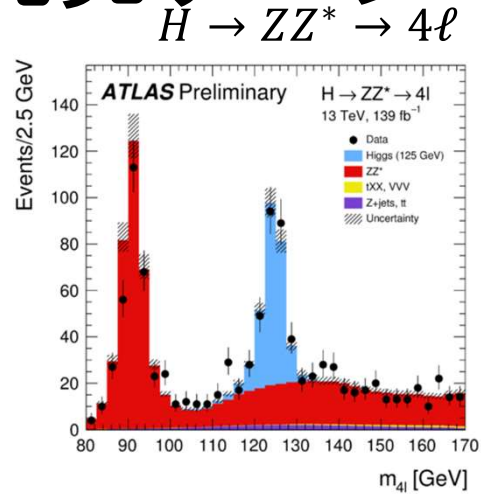
ATLAS-CONF-2019-025

現在では、 $H \rightarrow \gamma\gamma$, $H \rightarrow ZZ^* \rightarrow 4l$ チャンネルは大量の候補事象。

ヒッグス発見チャンネルの現在(2)



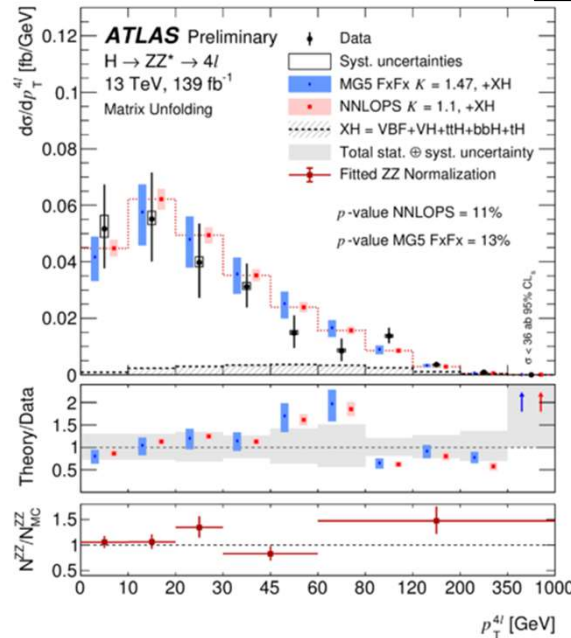
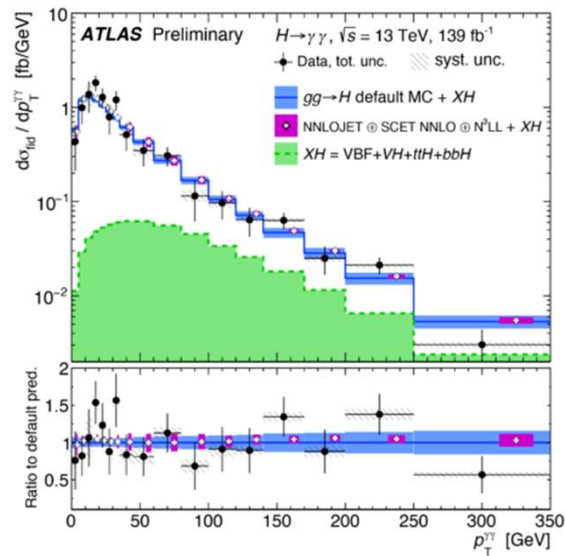
ATLAS-CONF-2019-032



ATLAS-CONF-2019-025

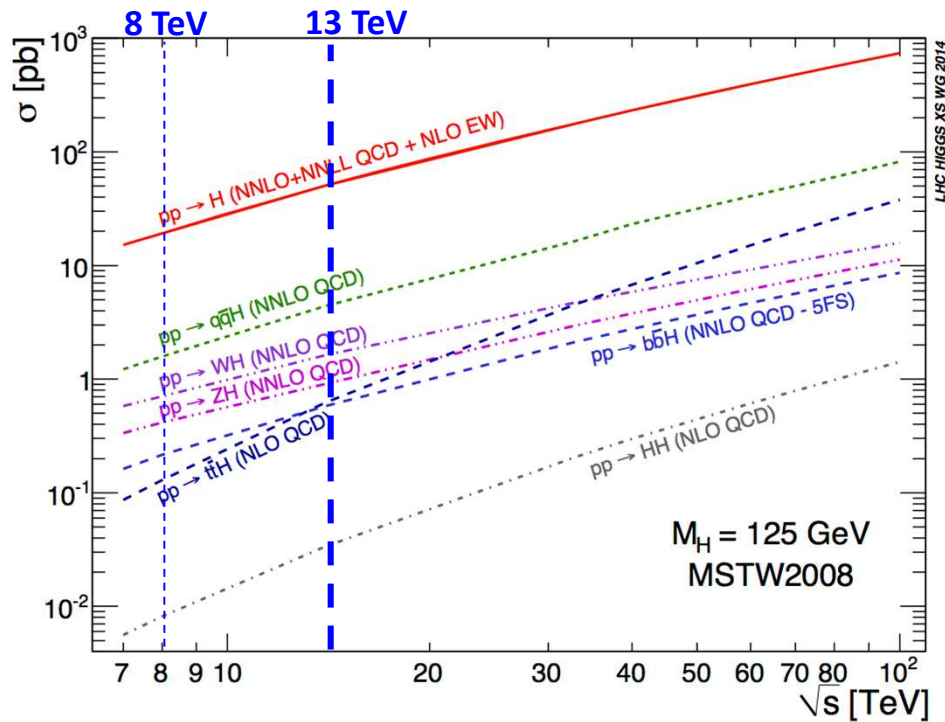
現在では、 $H \rightarrow \gamma\gamma, H \rightarrow ZZ^*$ チャンネルは大量の候補事象。

微分断面積を測定し、ヒッグス粒子事象の精査を続ける。



LHCでのヒッグス粒子の生成

- 生成断面積

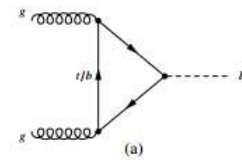


$\sigma_{gg \rightarrow H}$

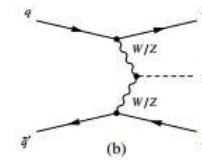
\sqrt{s} (TeV)	σ
13	48.61 pb
14	54.72 pb
27	146.65 pb

	$\sigma(14\text{TeV})/\sigma(8\text{TeV})$
$gg \rightarrow H$	2.6 ($M_X = M_H$)
$qq \rightarrow qqH$	2.6 (probes high M_X)
$qq \rightarrow VH$	2.1 ($M_X = M_V + M_H$)
$gg \rightarrow ttH$	4.7 (phase space + M_X)

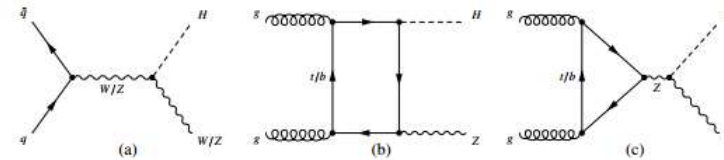
$gg \rightarrow H$



$qq \rightarrow qqH$



$qq \rightarrow VH$ Feynman diagrams for Higgs boson production via the (a) ggF and (b) VBF production



$gg \rightarrow ttH$ Feynman diagrams of Higgs boson production via the (a) $q\bar{q} \rightarrow VH$ and (b,c) $gg \rightarrow ZH$

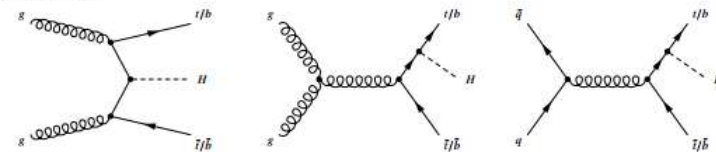
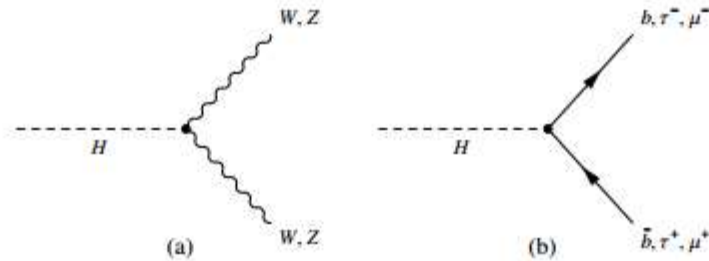


Figure 3: Leading-order Feynman diagrams of Higgs boson production via the $q\bar{q}/gg \rightarrow t\bar{t}H$ and $q\bar{q}/gg \rightarrow bbH$ processes.

ヒッグス粒子の崩壊

$H \rightarrow WW/ZZ$

$H \rightarrow \text{fermion pair}$



さまざまな生成・崩壊モード

- さまざまな測定を行い、標準理論を検証できる。

重心エネルギー 8 TeV \Rightarrow 13 TeV

- 生成断面積は、2-5倍。
- Run2では、たくさん作って様々なチャンネルで精密測定する。

Figure 5: Leading-order Feynman diagrams of Higgs boson decays (a) to W and Z bosons and (b) to fermions.

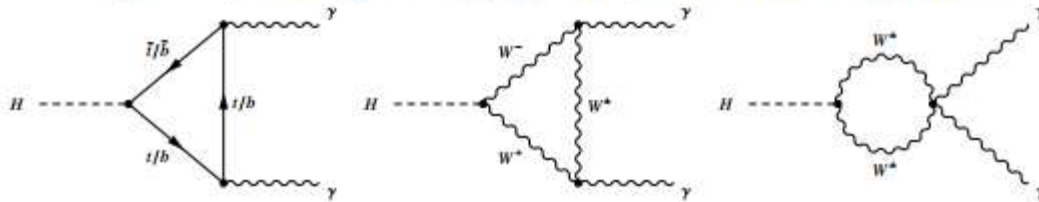


Figure 6: Leading-order Feynman diagrams of Higgs boson decays to a pair of photons.

- 崩壊分岐比 ($m_H = 125 \text{ GeV}$)

$H \rightarrow b\bar{b}$	$H \rightarrow \tau^+\tau^-$	$H \rightarrow \mu^+\mu^-$	$H \rightarrow c\bar{c}$
57.7%	6.32%	0.022%	2.91%

$H \rightarrow gg$	$H \rightarrow \gamma\gamma$	$H \rightarrow Z\gamma$	$H \rightarrow WW$	$H \rightarrow ZZ$	Γ_H [MeV]
8.6%	0.23%	0.15%	21.5%	2.64%	4.07

Run1での信号の有意度

3年ほど前のスライドから

ATLAS、CMS個別

Channel	References for individual publications		Signal strength [μ]		Signal significance [σ]	
	ATLAS	CMS	from results in this paper (Section 5.2)		ATLAS	CMS
			ATLAS	CMS		
$H \rightarrow \gamma\gamma$	[51]	[52]	$1.15^{+0.27}_{-0.25}$ (+0.26) (-0.24)	$1.12^{+0.25}_{-0.23}$ (+0.24) (-0.22)	5.0 (4.6)	5.6 (5.1)
$H \rightarrow ZZ \rightarrow 4\ell$	[53]	[54]	$1.51^{+0.39}_{-0.34}$ (+0.33) (-0.27)	$1.05^{+0.32}_{-0.27}$ (+0.31) (-0.26)	6.6 (5.5)	7.0 (6.8)
$H \rightarrow WW$	[55,56]	[57]	$1.23^{+0.23}_{-0.21}$ (+0.21) (-0.20)	$0.91^{+0.24}_{-0.21}$ (+0.23) (-0.20)	6.8 (5.8)	4.8 (5.6)
$H \rightarrow \tau\tau$	[58]	[59]	$1.41^{+0.40}_{-0.35}$ (+0.37) (-0.33)	$0.89^{+0.31}_{-0.28}$ (+0.31) (-0.29)	4.4 (3.3)	3.4 (3.7)
$H \rightarrow bb$	[38]	[39]	$0.62^{+0.37}_{-0.36}$ (+0.39) (-0.37)	$0.81^{+0.45}_{-0.42}$ (+0.45) (-0.43)	1.7 (2.7)	2.0 (2.5)
$H \rightarrow \mu\mu$	[60]	[61]	-0.7 ± 3.6 (± 3.6)	0.8 ± 3.5 (± 3.5)		
ttH production	[28,62,63]	[65]	$1.9^{+0.8}_{-0.7}$ (+0.72) (-0.66)	$2.9^{+1.0}_{-0.9}$ (+0.88) (-0.80)	2.7 (1.6)	3.6 (1.3)

3 σ : "兆候が見えた"
5 σ : "発見した"

- メインの生成・崩壊過程の多くはRun 1で発見がすんだ。
- ttH 生成、 $H \rightarrow bb$ はRun2で検証していく。
- LHC Run 2では、一個一個の過程の理解を確立し、精密測定に入っていく。

ATLAS+CMS

Production process	Measured significance (σ)	Expected significance (σ)
VBF	5.4	4.7
WH	2.4	2.7
ZH	2.3	2.9
VH	3.5	4.2
ttH	4.4	2.0
Decay channel		
$H \rightarrow \tau\tau$	5.5	5.0
$H \rightarrow bb$	2.6	3.7

Run1での信号の有意度

ATLAS、CMS個別

Channel	References for individual publications		Signal strength [μ]		Signal significance [σ]	
	ATLAS	CMS	from results in this paper (Section 5.2)		ATLAS	CMS
			ATLAS	CMS		
$H \rightarrow \gamma\gamma$	[51]	[52]	$1.15^{+0.27}_{-0.25}$ ($+0.26$, -0.24)	$1.12^{+0.25}_{-0.23}$ ($+0.24$, -0.22)	5.0 (4.6)	5.6 (5.1)
$H \rightarrow ZZ \rightarrow 4\ell$	[53]	[54]	$1.51^{+0.39}_{-0.34}$ ($+0.33$, -0.27)	$1.05^{+0.32}_{-0.27}$ ($+0.31$, -0.26)	6.6 (5.5)	7.0 (6.8)
$H \rightarrow WW$	[55, 56]	[57]	$1.23^{+0.23}_{-0.21}$ ($+0.21$, -0.20)	$0.91^{+0.24}_{-0.21}$ ($+0.23$, -0.20)	6.8 (5.8)	4.8 (5.6)
$H \rightarrow \tau\tau$	[58]	[59]	$1.41^{+0.40}_{-0.35}$ ($+0.37$, -0.33)	$0.89^{+0.31}_{-0.28}$ ($+0.31$, -0.29)	4.4 (3.3)	3.4 (3.7)
$H \rightarrow bb$	[38]	[39]	$0.62^{+0.37}_{-0.36}$ ($+0.39$, -0.37)	$0.81^{+0.45}_{-0.42}$ ($+0.45$, -0.43)	5.3 (2.7)	2.0 (2.5)
$H \rightarrow \mu\mu$	[60]	[61]	-0.7 ± 3.6 (± 3.6)	0.8 ± 3.5 (± 3.5)		
ttH production	[28, 62, 63]	[65]	$1.9^{+0.8}_{-0.7}$ ($+0.72$, -0.66)	$2.9^{+1.0}_{-0.9}$ ($+0.88$, -0.80)	5.8 (1.6)	3.6 (1.3)

3 σ : "兆候が見えた"

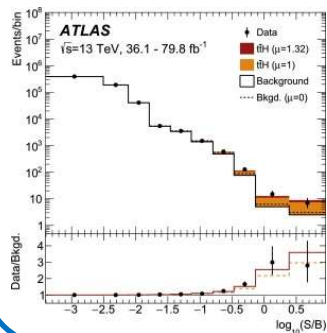
5 σ : "発見した"

- ゲージボソンと第三世代との結合は確立できた。
- 第2世代との結合、見えるか？

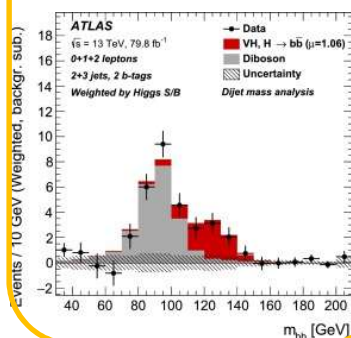
ATLAS+CMS

Production process	Measured significance (σ)	Expected significance (σ)
VBF	5.4	4.7
WH	2.4	2.7
ZH	2.3	2.9
VH	3.5	4.2
ttH	4.4	2.0
Decay channel		
$H \rightarrow \tau\tau$	5.5	5.0
$H \rightarrow bb$	2.6	3.7

ttH生成 5.8 σ Observation



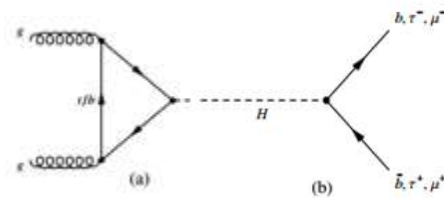
$H \rightarrow bb$ 崩壊 5.3 σ Observation



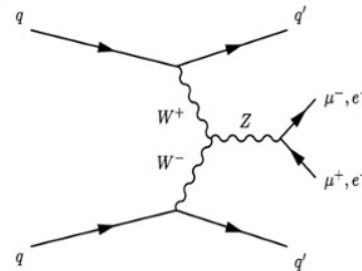
Search for $H \rightarrow \mu\mu$

- 第3世代 (τ, b, t)との湯川カップリングは確認できた。
- 第2世代粒子との湯川カップリングの発見を目指す
 - VBFに特化した信号領域を定義して解析感度を向上
 - 前後方dijet, high $m(jj)$ \Rightarrow VBFチャンネル

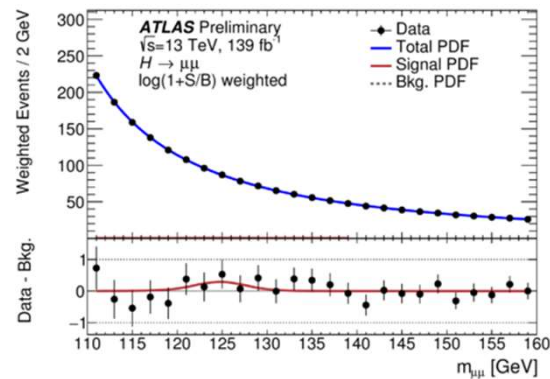
gg-fusion生成



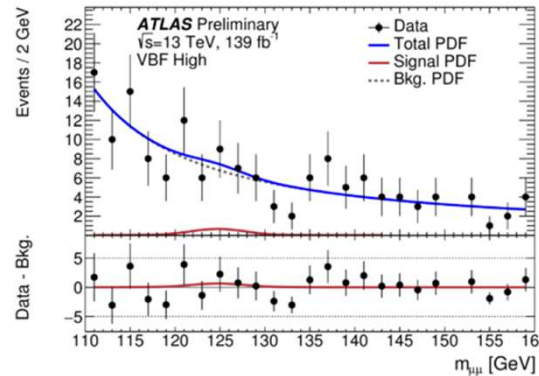
Vector Boson Fusion生成



all candidates (ggF+VBF)



VBF channel:



信号強度

$$\mu = \frac{(\sigma_H \times Br_{H \rightarrow \mu\mu})^{meas}}{(\sigma_H \times Br_{H \rightarrow \mu\mu})^{pred}} = 0.5 \pm 0.7$$

信号強度のリミット:

$$\mu < 1.7 \text{ (95\% CL)}$$

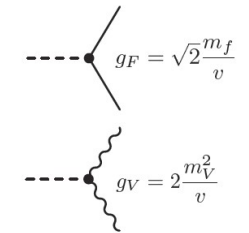
Higgs Coupling Measurement

$$L_h = \frac{1}{2}(\partial^\mu h)(\partial_\mu h) + \frac{M_h^2}{2} h^2 - \frac{M_h^2}{2v} h^3 - \frac{M_h^2}{8v^2} h^4$$

$$+ \left(M_W^2 W_\mu^+ W^{-\mu} + \frac{1}{2} M_Z^2 Z_\mu Z^\mu \right) \left(1 + \frac{h}{v} \right)^2$$

$$- \sum_f m_f \bar{f} f \left(1 + \frac{h}{v} \right).$$

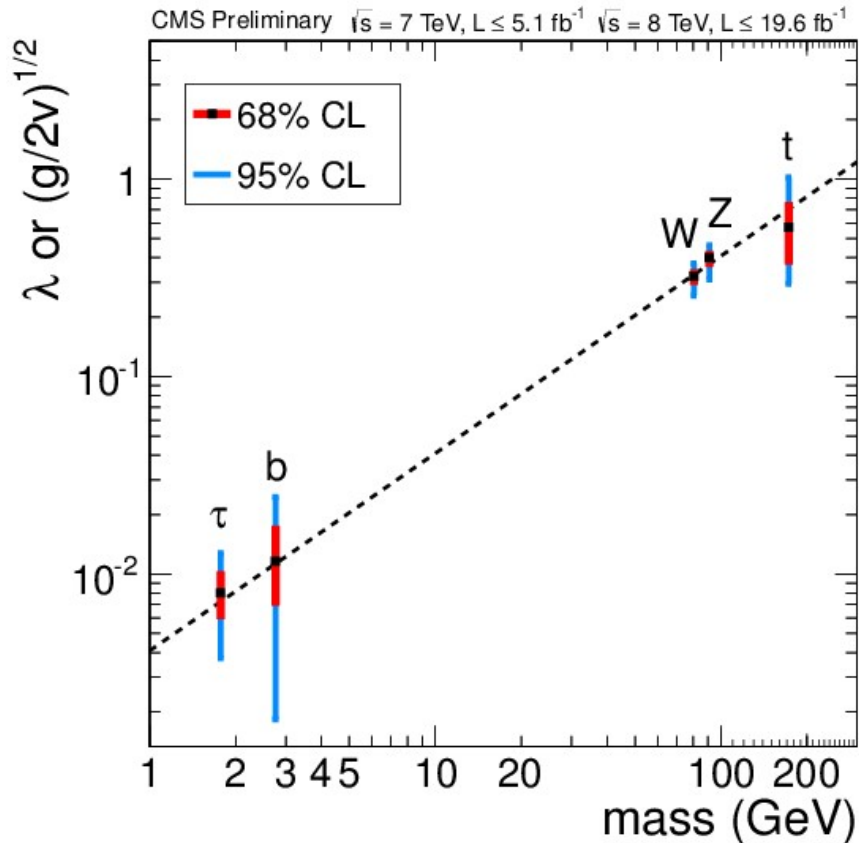
(19)



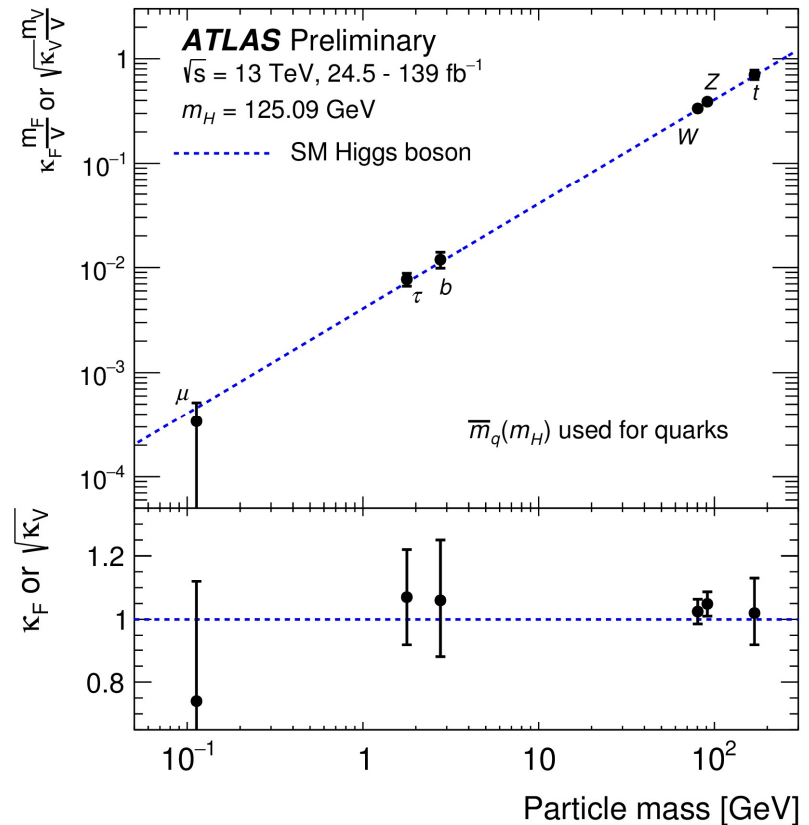
$$g_F^{meas} = \sqrt{2} \kappa_F \frac{m_f}{v}$$

$$g_V^{meas} = 2 \kappa_V \frac{m_V^2}{v}$$

Run 1 full data (CMS)

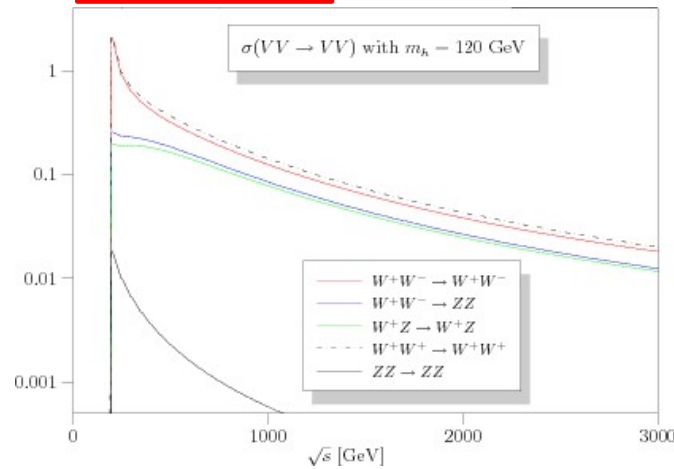
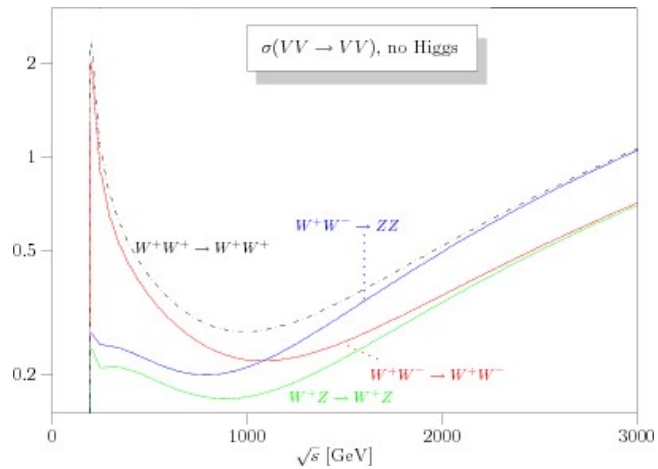
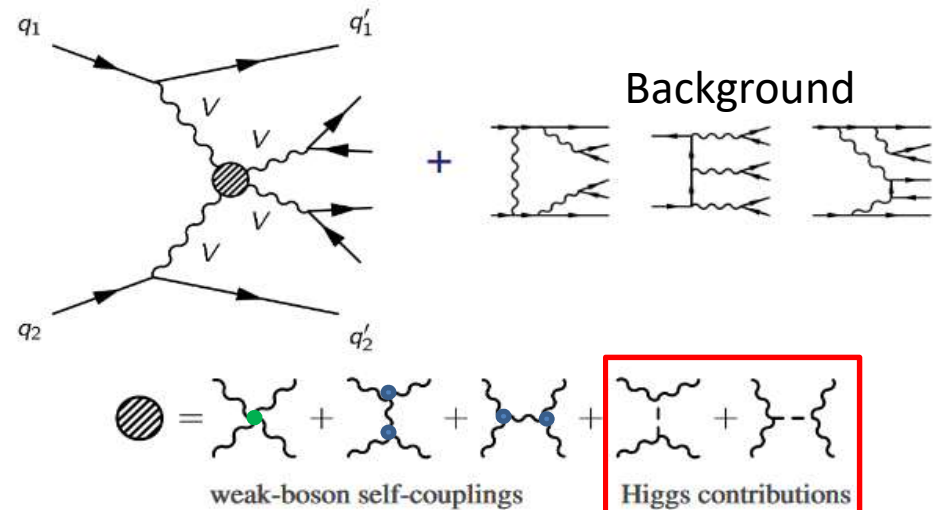


現在



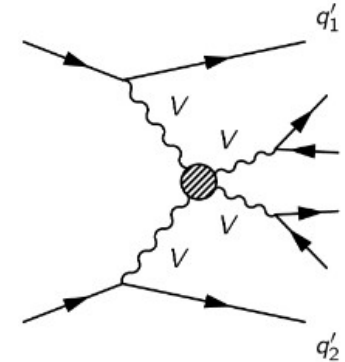
Vector Boson Scattering Processes

- Vector boson scattering involves
 - Triple and Quadratic Gauge Couplings
 - Higgs restores unitarity at high energies

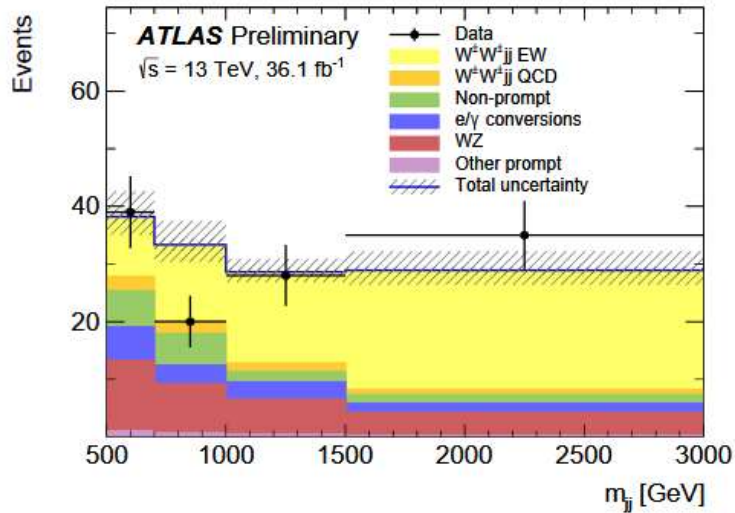


2018夏の結果

Vector Boson Scattering



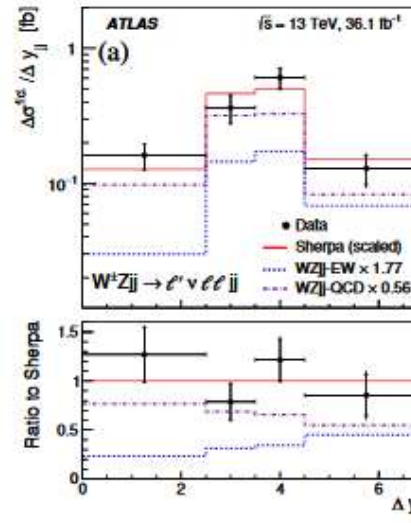
- 前後方にdijet + vector bosonの崩壊
- $W^\pm W^\pm jj \rightarrow \ell^\pm \ell^\pm + MET + jj$
- $WZjj \rightarrow 3\ell + jj$



$$\sigma^{EWK} = 2.91^{+0.51}_{-0.47} \text{ (stat.)} \pm 0.27 \text{ (sys.) fb}$$

6.9 σ observation
(expected 4.6 σ)

ATLAS-CONF-2018-030



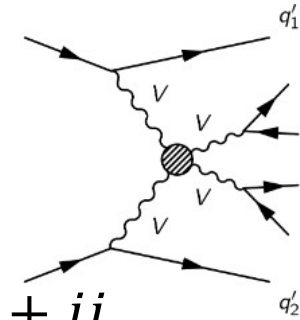
$$\sigma_{WZjj-EW} = 0.57^{+0.14}_{-0.13} \text{ (stat.)} \begin{matrix} +0.05 \\ -0.04 \end{matrix} \text{ (exp. syst.)} \begin{matrix} +0.05 \\ -0.04 \end{matrix} \text{ (mod. syst.)} \begin{matrix} +0.01 \\ -0.01 \end{matrix} \text{ (lumi.) fb.}$$

5.3 σ observation
(expected 3.2 σ)

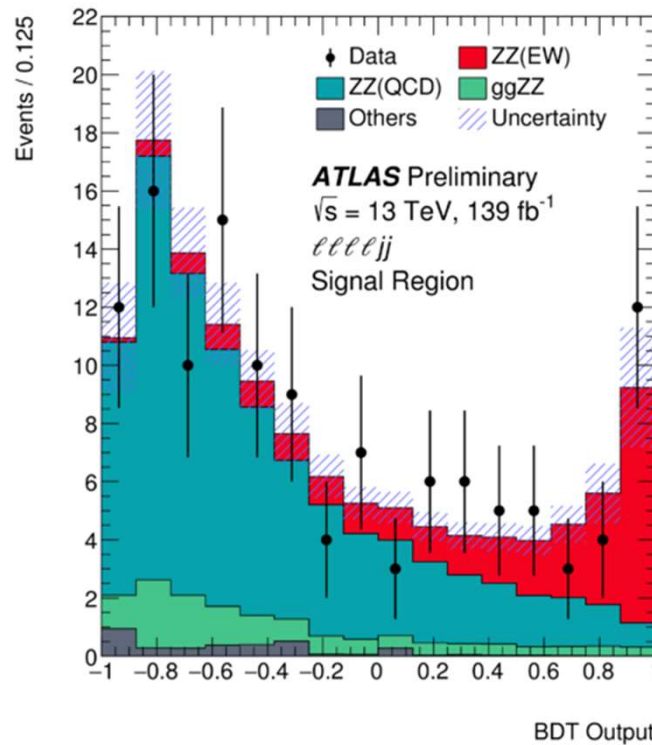
arXiv:1812.09740

VBSは、ちょうどプロセスが発見に達したところ。
これから、ヒッグスとの干渉について、精密検証を行う。

Vector Boson Scattering (2)



- $VVjj \rightarrow ZZjj \rightarrow 4\ell + jj$

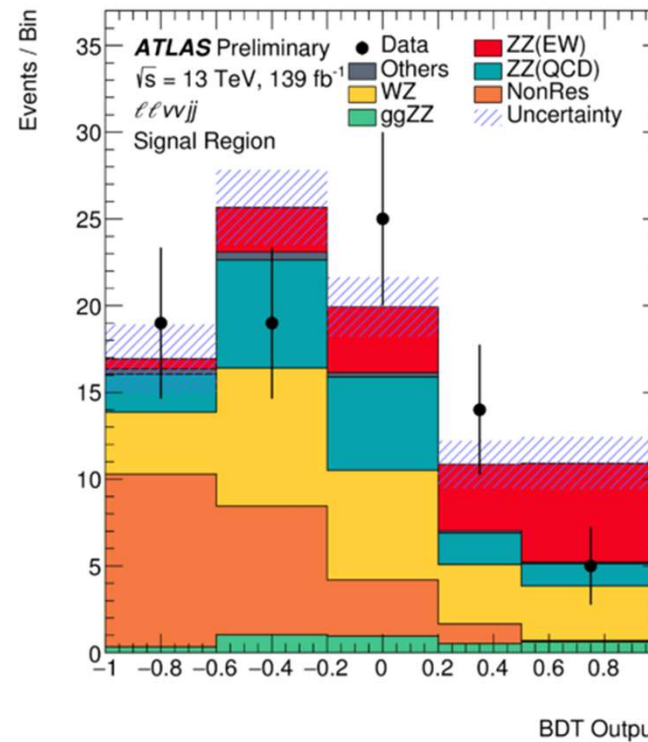


$$\sigma^{EWK} = 0.82 \pm 0.21 \text{ fb}$$

5.5 σ observation (expected 4.3 σ)

VBSは、WW,WZ,ZZの終状態が観測に達した。
これから、ヒッグスとの干渉について、精密検証を行う。

- $VVjj \rightarrow ZZjj \rightarrow \ell^+ \ell^- + 2\nu + jj$



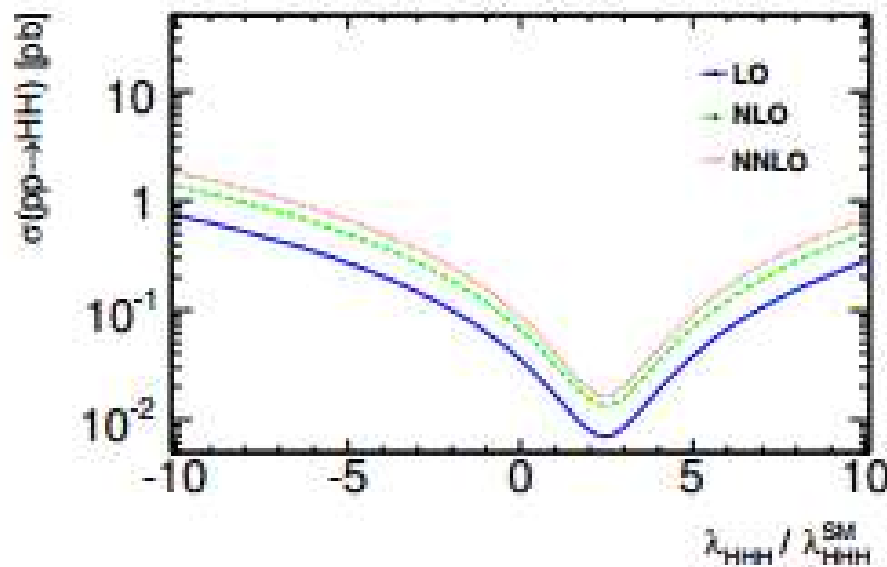
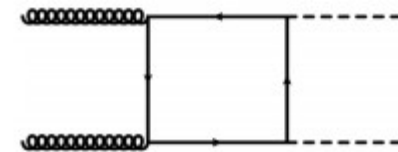
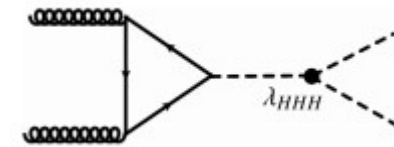
ATLAS-CONF-2019-033

D2 若狭

$VVjj \rightarrow WVjj \rightarrow semileptonic$

ヒッグス自己結合測定

- DiHiggs事象を探して解析する。
- DiHiggsは、2つのダイアグラムの干渉が起こる。
- もし自己相互作用(λ_{HHH})がなければ、HH生成の断面積は2倍になる。



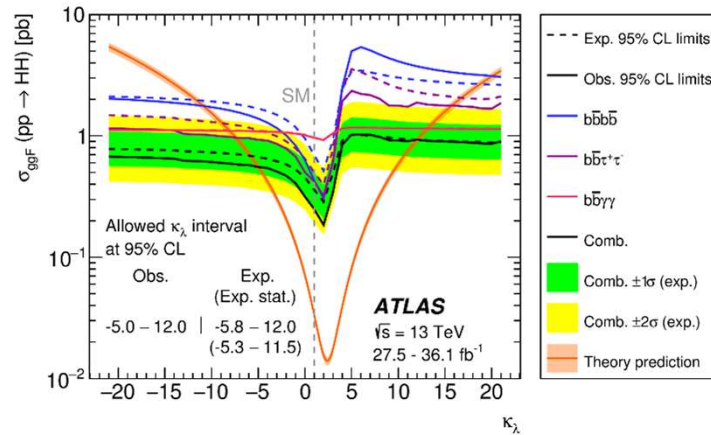
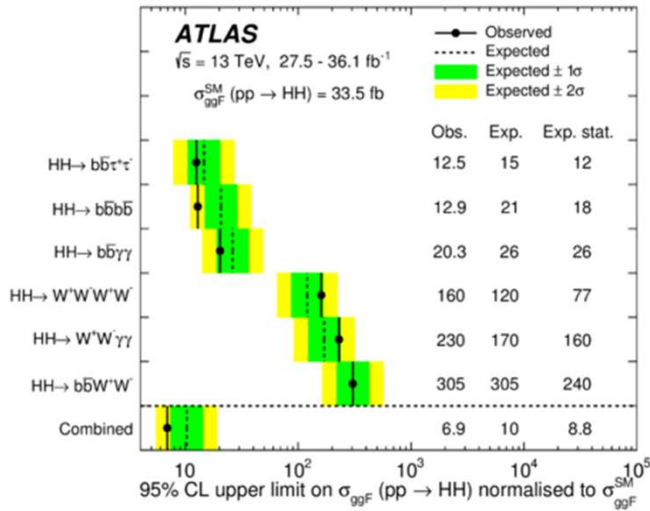
Expected event yields for $\frac{\lambda_{HHH}}{\lambda_{SM}} = 1$

Decay Channel	Branching Ratio	Total Yield (3000 fb ⁻¹)
$b\bar{b} + b\bar{b}$	33%	40,000
$b\bar{b} + W^+W^-$	25%	31,000
$b\bar{b} + \tau^+\tau^-$	7.3%	8,900
$ZZ + b\bar{b}$	3.1%	3,800
$W^+W^- + \tau^+\tau^-$	2.7%	3,300
$ZZ + W^+W^-$	1.1%	1,300
$\gamma\gamma + b\bar{b}$	0.26%	320
$\gamma\gamma + \gamma\gamma$	0.0010%	1.2

Run 2でのDihiggs探索結果

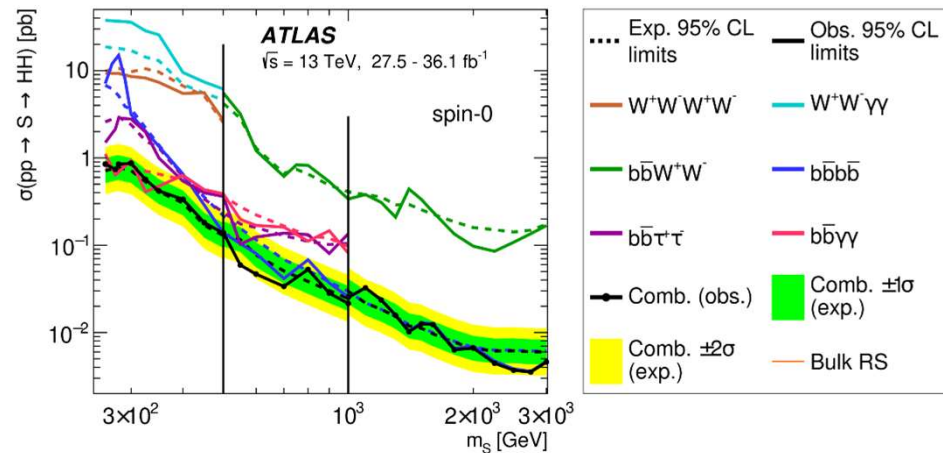
- まずはDihiggs事象を探している。

Dihiggs事象の生成断面積に対する上限 自己相互結合に対する制限



$-5.0 < \kappa_\lambda < 12.1$ at 95% CL.

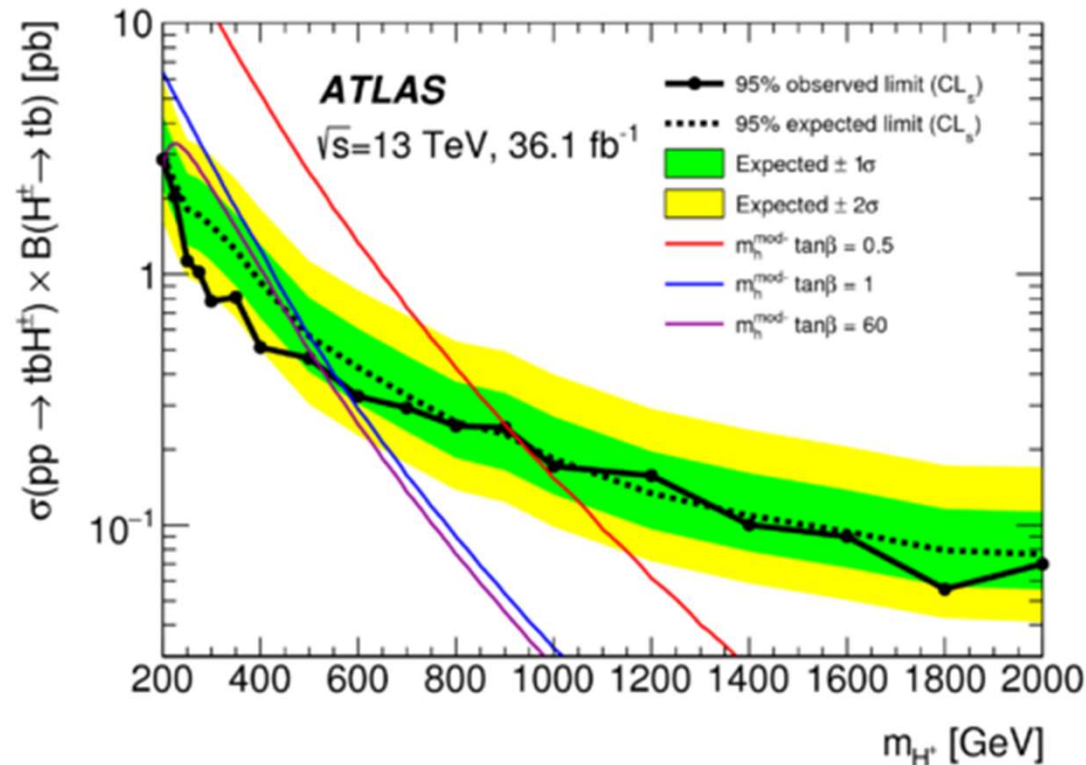
$S \rightarrow hh$ 事象の探索として、
同じデータを解釈することも
できる:
(e.g. S =heavy Higgs)



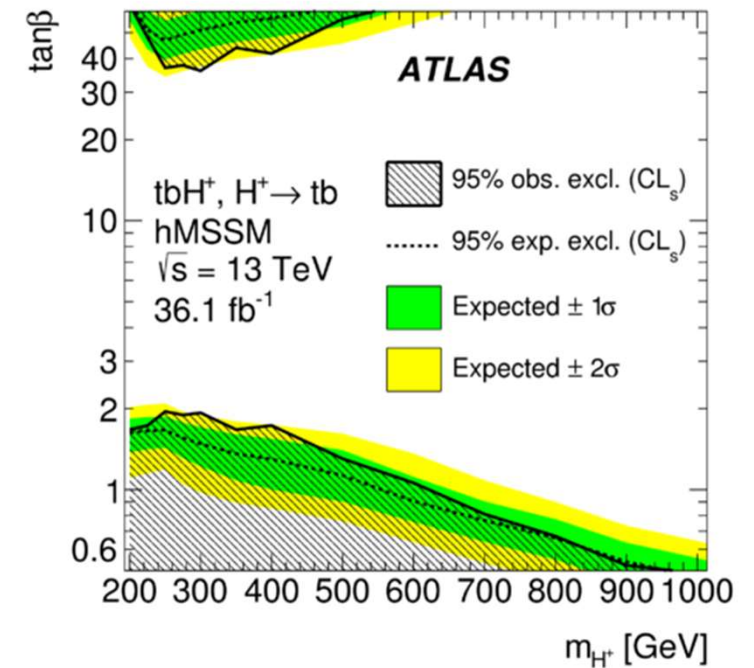
荷電ヒッグス粒子に対する制約

- 荷電ヒッグス粒子の信号は見つからず、データはバックグラウンドとよく一致した。

生成断面積に対する制約



MSSM (hMSSMシナリオ) に対する制約



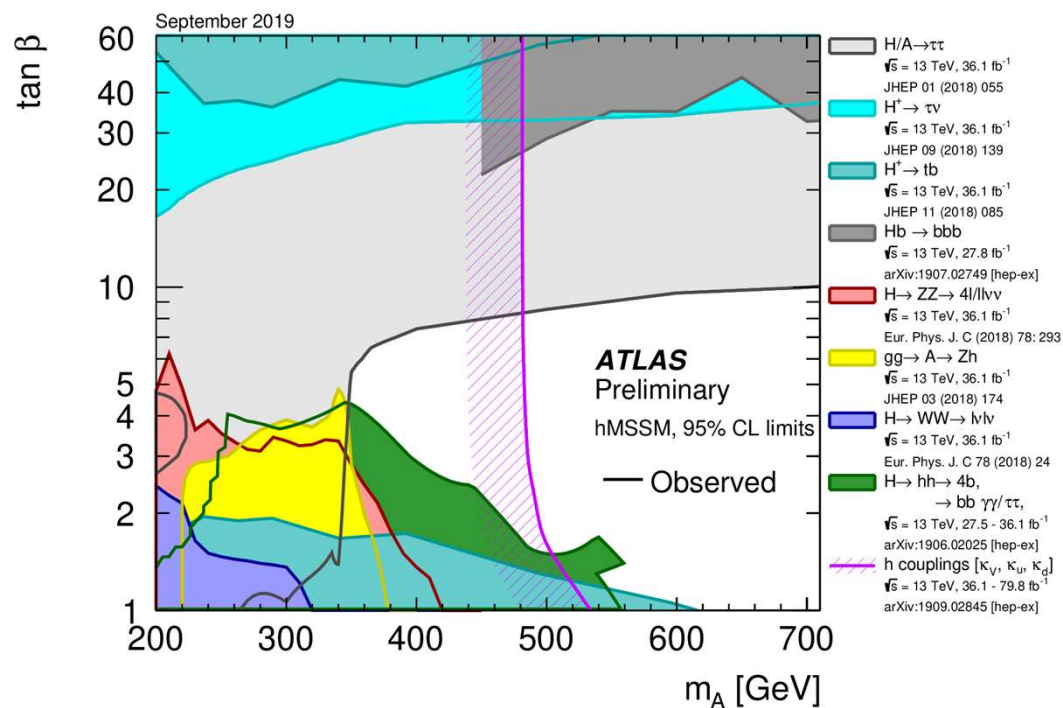
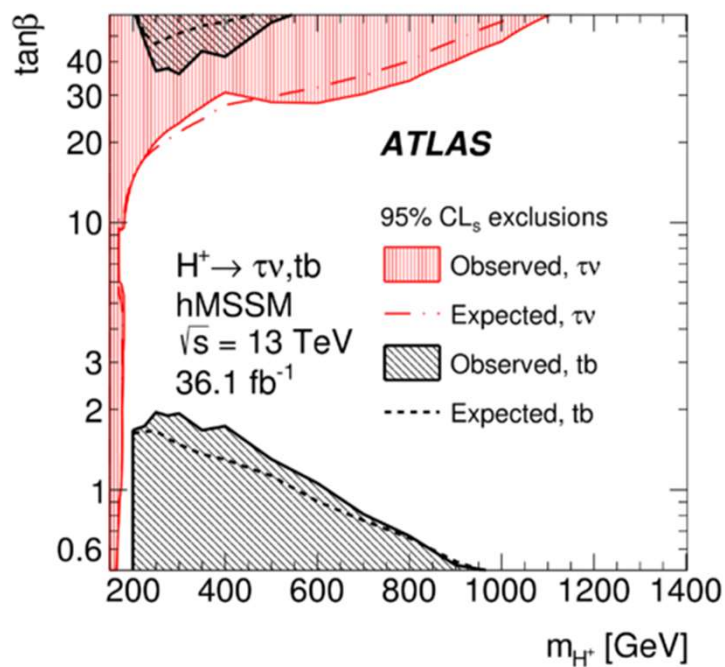
D1 山内

$H^+ \rightarrow \tau\nu$ チャンネルとの比較

- $H^+ \rightarrow \tau\nu$ チャンネルとは、感度のある領域が異なるため、MSSMの解析という意味でも相補的といえる。

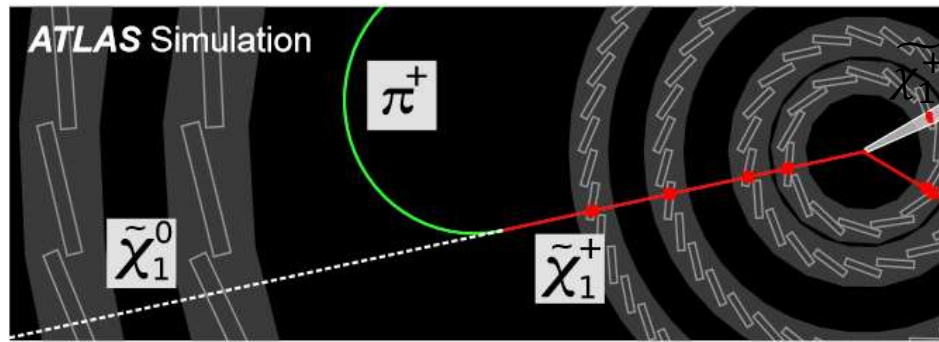
[JHEP 11 \(2018\) 085](#)

ATLASでのMSSMヒッグス探索のまとめ

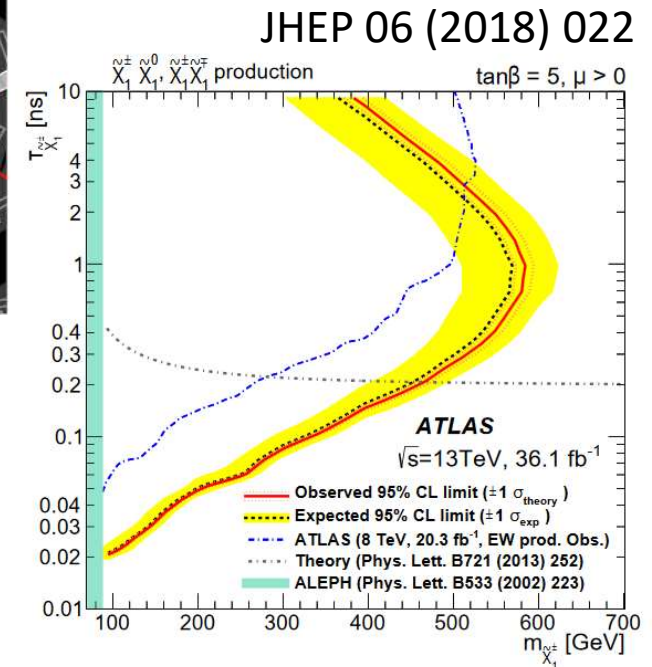
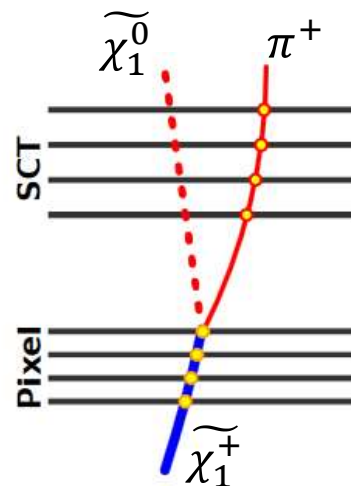
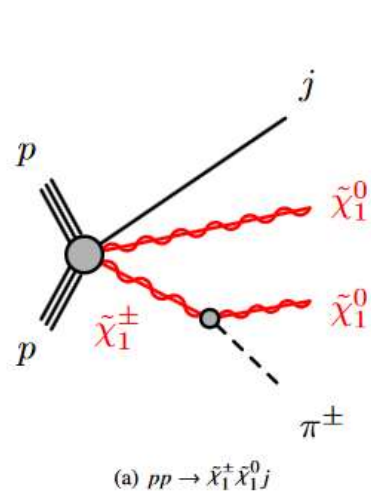


Long Lived Chargino

- WinoがLSPの場合に、 $\tilde{\chi}_1^+$, $\tilde{\chi}_1^0$ の質量が縮退する場合がある。
 - AMSBでは、この $\tilde{\chi}_1^0$ がDMになりうる。
- $\tilde{\chi}_0^+$ は長寿命→Long Lived Particle (LLP)になる。



~30cm



ATLAS Supersymmetry Searches

ATLAS SUSY Searches* - 95% CL Lower Limits
October 2019

ATLAS Preliminary
 $\sqrt{s} = 13$ TeV

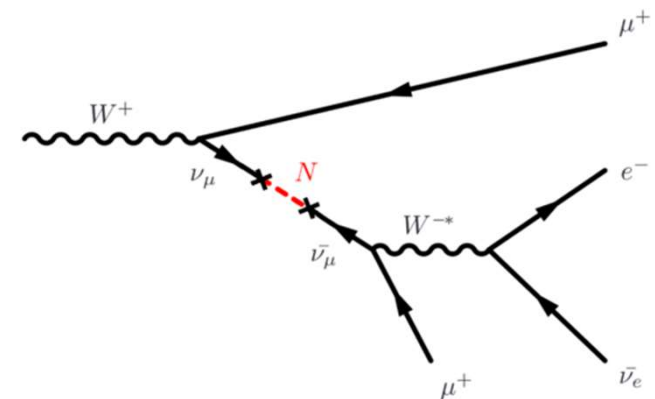
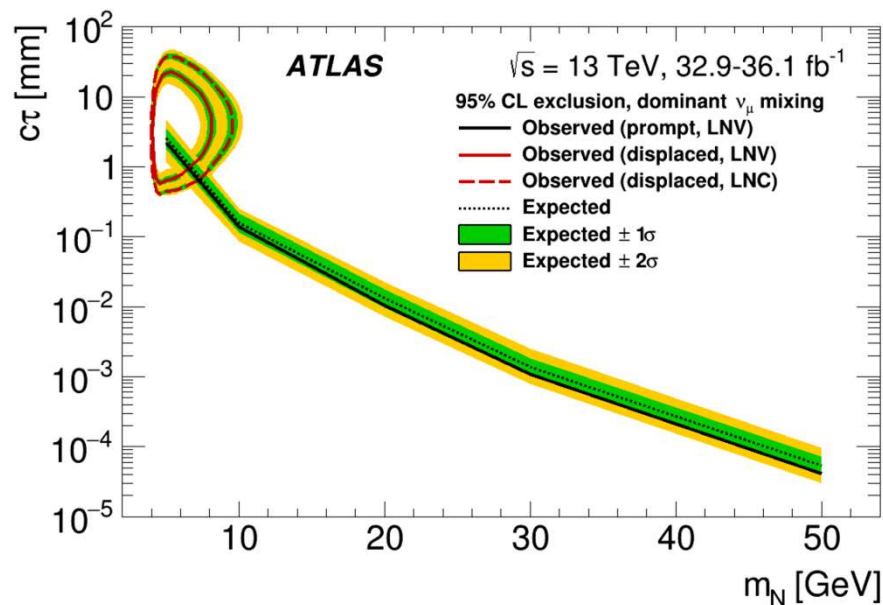
	Model	Signature	$\int \mathcal{L} dt$ [fb ⁻¹]	Mass limit	Reference					
Inclusive Searches	$\tilde{q}\tilde{q}, \tilde{q} \rightarrow q\tilde{\chi}_1^0$	0 e, μ mono-jet	2-6 jets 1-3 jets	E_T^{miss} E_T^{miss}	139 36.1	\tilde{q} [10x Degen.] \tilde{q} [1x, 8x Degen.]	1.9 0.43 0.71	$m(\tilde{\chi}_1^0) < 400$ GeV $m(\tilde{q}) - m(\tilde{\chi}_1^0) = 5$ GeV	ATLAS-CONF-2019-040 1711.03301	
	$\tilde{g}\tilde{g}, \tilde{g} \rightarrow q\tilde{q}\tilde{\chi}_1^0$	0 e, μ	2-6 jets	E_T^{miss}	139	\tilde{g} \tilde{g}	2.35 Forbidden 1.15-1.95	$m(\tilde{\chi}_1^0) = 0$ GeV $m(\tilde{g}) = 1000$ GeV	ATLAS-CONF-2019-040 ATLAS-CONF-2019-040	
	$\tilde{g}\tilde{g}, \tilde{g} \rightarrow q\tilde{q}(\ell\ell)\tilde{\chi}_1^0$	3 e, μ $ee, \mu\mu$	4 jets 2 jets	E_T^{miss} E_T^{miss}	36.1 36.1	\tilde{g} \tilde{g}	1.2 1.85	$m(\tilde{\chi}_1^0) < 800$ GeV $m(\tilde{g}) - m(\tilde{\chi}_1^0) = 50$ GeV	1706.03731 1805.11381	
	$\tilde{g}\tilde{g}, \tilde{g} \rightarrow qqWZ\tilde{\chi}_1^0$	0 e, μ SS e, μ	7-11 jets 6 jets	E_T^{miss} E_T^{miss}	36.1 139	\tilde{g} \tilde{g}	1.15 1.8	$m(\tilde{\chi}_1^0) < 400$ GeV $m(\tilde{g}) - m(\tilde{\chi}_1^0) = 200$ GeV	1708.02794 1909.08457	
	$\tilde{g}\tilde{g}, \tilde{g} \rightarrow t\tilde{\chi}_1^0$	0-1 e, μ SS e, μ	3 b 6 jets	E_T^{miss} E_T^{miss}	79.8 139	\tilde{g} \tilde{g}	2.25 1.25	$m(\tilde{\chi}_1^0) < 200$ GeV $m(\tilde{g}) - m(\tilde{\chi}_1^0) = 300$ GeV	ATLAS-CONF-2018-041 ATLAS-CONF-2019-015	
	3 rd gen. squarks direct production	$\tilde{b}_1\tilde{b}_1, \tilde{b}_1 \rightarrow b\tilde{\chi}_1^0 / t\tilde{\chi}_1^\pm$	Multiple Multiple Multiple	Multiple Multiple Multiple	E_T^{miss} E_T^{miss} E_T^{miss}	36.1 36.1 139	\tilde{b}_1 \tilde{b}_1 \tilde{b}_1	Forbidden Forbidden 0.58-0.82 Forbidden 0.74	$m(\tilde{\chi}_1^0) = 300$ GeV, $BR(\tilde{b}_1 \rightarrow t\tilde{\chi}_1^\pm) = 1$ $m(\tilde{\chi}_1^0) = 300$ GeV, $BR(\tilde{b}_1 \rightarrow b\tilde{\chi}_1^0) = BR(\tilde{b}_1 \rightarrow t\tilde{\chi}_1^\pm) = 0.5$ $m(\tilde{\chi}_1^0) = 200$ GeV, $m(\tilde{b}_1) = 300$ GeV, $BR(\tilde{b}_1 \rightarrow t\tilde{\chi}_1^\pm) = 1$	1708.09266, 1711.03301 1708.09266 ATLAS-CONF-2019-015
$\tilde{b}_1\tilde{b}_1, \tilde{b}_1 \rightarrow b\tilde{\chi}_2^0 \rightarrow bh\tilde{\chi}_1^0$		0 e, μ	6 b	E_T^{miss}	139	\tilde{b}_1 \tilde{b}_1	Forbidden 0.23-0.48	$\Delta m(\tilde{\chi}_2^0, \tilde{\chi}_1^0) = 130$ GeV, $m(\tilde{\chi}_1^0) = 100$ GeV $\Delta m(\tilde{\chi}_2^0, \tilde{\chi}_1^0) = 130$ GeV, $m(\tilde{\chi}_1^0) = 0$ GeV	1908.03122 1908.03122	
$\tilde{t}_1\tilde{t}_1, \tilde{t}_1 \rightarrow Wb\tilde{\chi}_1^0$ or $t\tilde{\chi}_1^0$		0-2 e, μ	0-2 jets/1-2 b	E_T^{miss}	36.1	\tilde{t}_1	1.0	$m(\tilde{\chi}_1^0) = 1$ GeV	1506.08616, 1709.04183, 1711.11520	
$\tilde{t}_1\tilde{t}_1, \tilde{t}_1 \rightarrow Wb\tilde{\chi}_1^0$		1 e, μ	3 jets/1 b	E_T^{miss}	139	\tilde{t}_1	0.44-0.59	$m(\tilde{\chi}_1^0) = 400$ GeV	ATLAS-CONF-2019-017	
$\tilde{t}_1\tilde{t}_1, \tilde{t}_1 \rightarrow \tilde{\tau}_1 b\nu, \tilde{\tau}_1 \rightarrow \tau\tilde{G}$		1 $\tau + 1 e, \mu, \tau$	2 jets/1 b	E_T^{miss}	36.1	\tilde{t}_1	1.16	$m(\tilde{\tau}_1) = 800$ GeV	1803.10178	
$\tilde{t}_1\tilde{t}_1, \tilde{t}_1 \rightarrow c\tilde{\chi}_1^0 / \tilde{c}\tilde{c}, \tilde{c} \rightarrow c\tilde{\chi}_1^0$		0 e, μ	2 c	E_T^{miss}	36.1	\tilde{t}_1 \tilde{t}_1	0.85 0.46 0.43	$m(\tilde{\chi}_1^0) = 0$ GeV $m(\tilde{t}_1, \tilde{c}) - m(\tilde{\chi}_1^0) = 50$ GeV $m(\tilde{t}_1, \tilde{c}) - m(\tilde{\chi}_1^0) = 5$ GeV	1805.01649 1805.01649 1711.03301	
$\tilde{t}_2\tilde{t}_2, \tilde{t}_2 \rightarrow \tilde{t}_1 + h$		1-2 e, μ	4 b	E_T^{miss}	36.1	\tilde{t}_2	0.32-0.88	$m(\tilde{\chi}_1^0) = 0$ GeV, $m(\tilde{t}_1) - m(\tilde{\chi}_1^0) = 180$ GeV	1706.03986	
$\tilde{t}_2\tilde{t}_2, \tilde{t}_2 \rightarrow \tilde{t}_1 + Z$		3 e, μ	1 b	E_T^{miss}	139	\tilde{t}_2	Forbidden 0.86	$m(\tilde{\chi}_1^0) = 360$ GeV, $m(\tilde{t}_1) - m(\tilde{\chi}_1^0) = 40$ GeV	ATLAS-CONF-2019-016	
EW direct		$\tilde{\chi}_1^\pm\tilde{\chi}_2^0$ via WZ	2-3 e, μ $ee, \mu\mu$	≥ 1	E_T^{miss} E_T^{miss}	36.1 139	$\tilde{\chi}_1^\pm/\tilde{\chi}_2^0$ $\tilde{\chi}_1^\pm/\tilde{\chi}_2^0$	0.6 0.205	$m(\tilde{\chi}_1^0) = 0$ $m(\tilde{\chi}_1^\pm) - m(\tilde{\chi}_1^0) = 5$ GeV	1403.5294, 1806.02293 ATLAS-CONF-2019-014
		$\tilde{\chi}_1^\pm\tilde{\chi}_1^\mp$ via WW	2 e, μ		E_T^{miss}	139	$\tilde{\chi}_1^\pm$	0.42	$m(\tilde{\chi}_1^0) = 0$	1908.08215
	$\tilde{\chi}_1^\pm\tilde{\chi}_2^0$ via Wh	0-1 e, μ	2 $b/2 \gamma$	E_T^{miss}	139	$\tilde{\chi}_1^\pm/\tilde{\chi}_2^0$	Forbidden 0.74	$m(\tilde{\chi}_1^0) = 70$ GeV	ATLAS-CONF-2019-019, 1909.09226	
	$\tilde{\chi}_1^\pm\tilde{\chi}_1^\mp$ via $\tilde{\ell}_L/\tilde{\nu}$	2 e, μ		E_T^{miss}	139	$\tilde{\chi}_1^\pm$	1.0	$m(\tilde{\ell}, \tilde{\nu}) = 0.5(m(\tilde{\chi}_1^\pm) + m(\tilde{\chi}_1^0))$	ATLAS-CONF-2019-008	
	$\tilde{\tau}\tilde{\tau}, \tilde{\tau} \rightarrow \tau\tilde{\chi}_1^0$	2 τ		E_T^{miss}	139	$\tilde{\tau}$ [$\tilde{\tau}_L, \tilde{\tau}_{R,I}$]	0.16-0.3 0.12-0.39	$m(\tilde{\chi}_1^0) = 0$	ATLAS-CONF-2019-018	
	$\tilde{\ell}_{L,R}\tilde{\ell}_{L,R}, \tilde{\ell} \rightarrow \ell\tilde{\chi}_1^0$	2 e, μ 2 e, μ	0 jets ≥ 1	E_T^{miss} E_T^{miss}	139 139	$\tilde{\ell}$ $\tilde{\ell}$	0.7 0.256	$m(\tilde{\chi}_1^0) = 0$ $m(\tilde{\ell}) - m(\tilde{\chi}_1^0) = 10$ GeV	ATLAS-CONF-2019-008 ATLAS-CONF-2019-014	
	$\tilde{H}\tilde{H}, \tilde{H} \rightarrow h\tilde{G}/Z\tilde{G}$	0 e, μ 4 e, μ	$\geq 3 b$ 0 jets	E_T^{miss} E_T^{miss}	36.1 36.1	\tilde{H} \tilde{H}	0.13-0.23 0.3	$BR(\tilde{H} \rightarrow h\tilde{G}) = 1$ $BR(\tilde{H} \rightarrow Z\tilde{G}) = 1$	1806.04030 1804.03602	
Long-lived particles	Direct $\tilde{\chi}_1^\pm\tilde{\chi}_1^\mp$ prod., long-lived $\tilde{\chi}_1^\pm$	Disapp. trk	1 jet	E_T^{miss}	36.1	$\tilde{\chi}_1^\pm$ $\tilde{\chi}_1^\pm$	0.46 0.15	Pure Wino Pure Higgsino	1712.02118 ATL-PHYS-PUB-2017-019	
	Stable \tilde{g} R-hadron	Multiple	Multiple		36.1	\tilde{g}	2.0		1902.01636, 1808.04095	
	Metastable \tilde{g} R-hadron, $\tilde{g} \rightarrow qq\tilde{\chi}_1^0$	Multiple	Multiple		36.1	\tilde{g} [$\tau(\tilde{g}) = 10$ ns, 0.2 ns]	2.05 2.4	$m(\tilde{\chi}_1^0) = 100$ GeV	1710.04901, 1808.04095	
RPV	LFV $pp \rightarrow \tilde{\nu}_\tau + X, \tilde{\nu}_\tau \rightarrow e\mu/\tau\mu$	$e\mu, e\tau, \mu\tau$			3.2	$\tilde{\nu}_\tau$	1.9	$\lambda'_{311} = 0.11, \lambda'_{132}/\lambda'_{233} = 0.07$	1607.08079	
	$\tilde{\chi}_1^\pm\tilde{\chi}_1^\mp/\tilde{\chi}_2^0 \rightarrow WW/Z\ell\ell\nu\nu$	4 e, μ	0 jets	E_T^{miss}	36.1	$\tilde{\chi}_1^\pm/\tilde{\chi}_2^0$ [$\lambda'_{333} \neq 0, \lambda'_{124} \neq 0$]	0.82 1.33	$m(\tilde{\chi}_1^0) = 100$ GeV	1804.03602	
	$\tilde{g}\tilde{g}, \tilde{g} \rightarrow qq\tilde{\chi}_1^0, \tilde{\chi}_1^0 \rightarrow qq\tilde{\chi}_1^0$	4-5 large- R jets	Multiple		36.1 36.1	\tilde{g} [$m(\tilde{V}_1^0) = 200$ GeV, 1100 GeV] $\tilde{\chi}_1^0$ [$\lambda'_{112} = 2e-4, 2e-5$]	1.3 1.9 1.05 2.0	Large λ'_{112} $m(\tilde{\chi}_1^0) = 200$ GeV, bino-like	1804.03568 ATLAS-CONF-2018-003	
	$\tilde{t}, \tilde{t} \rightarrow t\tilde{\chi}_1^0, \tilde{\chi}_1^0 \rightarrow tbs$	Multiple	Multiple		36.1	\tilde{g} [$\lambda'_{323} = 2e-4, 1e-2$]	0.55 1.05	$m(\tilde{\chi}_1^0) = 200$ GeV, bino-like	ATLAS-CONF-2018-003	
	$\tilde{t}_1\tilde{t}_1, \tilde{t}_1 \rightarrow bs$	2 jets + 2 b			36.7	\tilde{t}_1 [qq, bs]	0.42 0.61		1710.07171	
	$\tilde{t}_1\tilde{t}_1, \tilde{t}_1 \rightarrow q\ell$	2 e, μ 1 μ	2 b DV		36.1 136	\tilde{t}_1 \tilde{t}_1	0.4-1.45 1.0 1.6	$BR(\tilde{t}_1 \rightarrow b\ell/h\nu) > 20\%$ $BR(\tilde{t}_1 \rightarrow q\mu) = 100\%, \cos\theta_t = 1$	1710.05544 ATLAS-CONF-2019-006	

*Only a selection of the available mass limits on new states or phenomena is shown. Many of the limits are based on simplified models, c.f. refs. for the assumptions made.

10⁻¹ 1 Mass scale [TeV]

Long Lived Heavy Neutral Lepton Search

- Search for right handed majorana neutrino (N or HNL)
 - Production and decay: function of m_N and coupling strength $|U|^2$
- A trigger muon w/ $p_T > 28 \text{ GeV}$ (prompt)
- DV (Displaced Vertex) with two leptons
 - $4 < r_{DV} < 300 \text{ mm}$
 - $m_{DV} > 4 \text{ GeV}$
- Background: hadron interaction w/ material, metastable b- and s-hadrons, accidental crossing particles, cosmic ray.



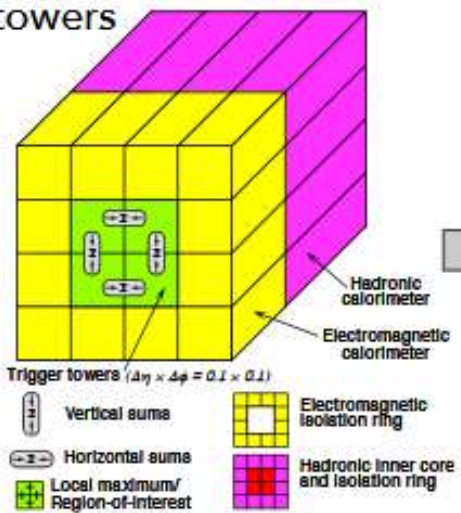
D1 和田

バックアップ

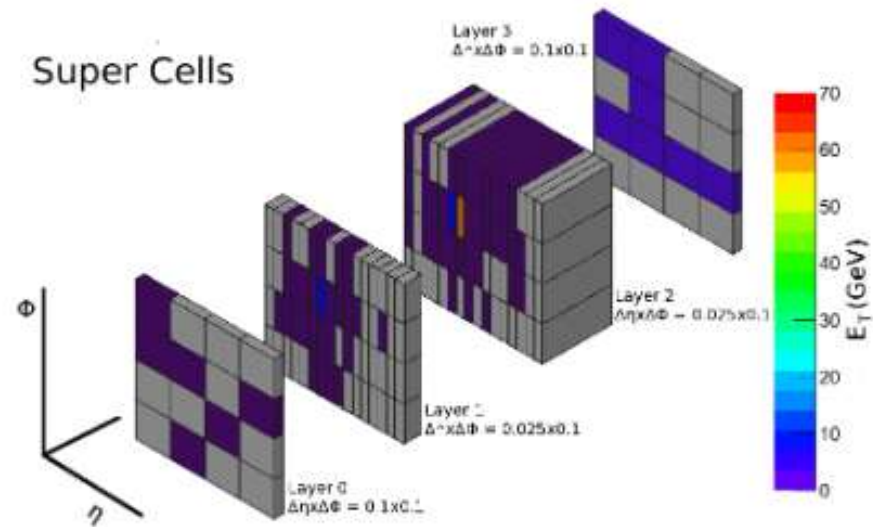
Super Cells

▶ Trigger tower ⇒ 10 Super Cells (SCs)

Trigger towers



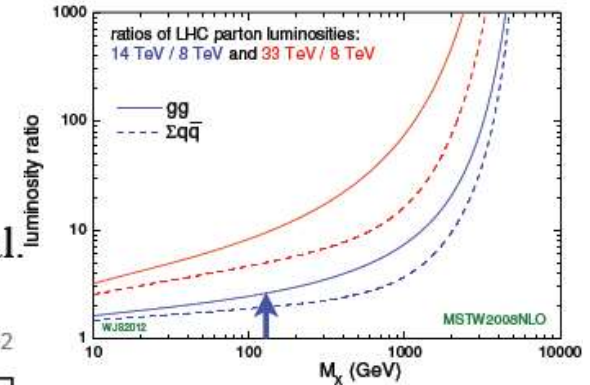
Super Cells



	Elementary Cell	Trigger Tower		Super Cell	
Layer (barrel)	$[\Delta\eta \times \Delta\phi]$	$[n_\eta \times n_\phi]$	$[\Delta\eta \times \Delta\phi]$	$[n_\eta \times n_\phi]$	$[\Delta\eta \times \Delta\phi]$
Presampler (layer 0)	0.025×0.1	4×1	0.1×0.1	4×1	0.1×0.1
Front (layer 1)	0.003125×0.1	32×1		8×1	0.025×0.1
Middle (layer 2)	0.025×0.025	4×4		1×4	0.025×0.1
Back (layer 3)	0.05×0.025	2×4		2×4	0.1×0.1

High Luminosity LHC (HL-LHC)

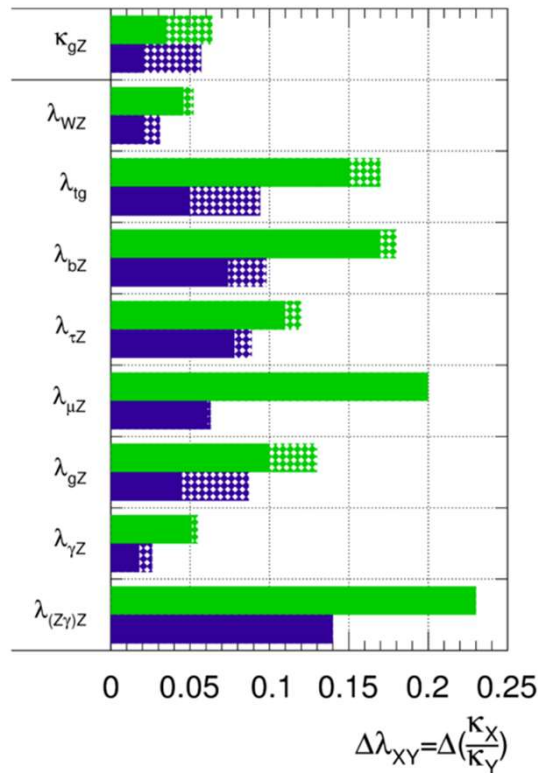
- ECFA HL-LHC with $L=300 \text{ fb}^{-1}$ (3 ab^{-1}) physics study.
- Higgs mass precision $\Delta M_H \sim 100$ (50) MeV.
- Access to top-Yukawa coupling via ttH , and rare decay $H \rightarrow \mu\mu$.
- Coupling precision of 10 to 5% reachable (even few% in κ_V/κ_Z).
- Detector performances (trigger, lepton-id, fake, τ/b -id) are crucial.
- Theory uncertainty dominates - challenge for theorists!



ATL-PHYS-PUB-2014-016

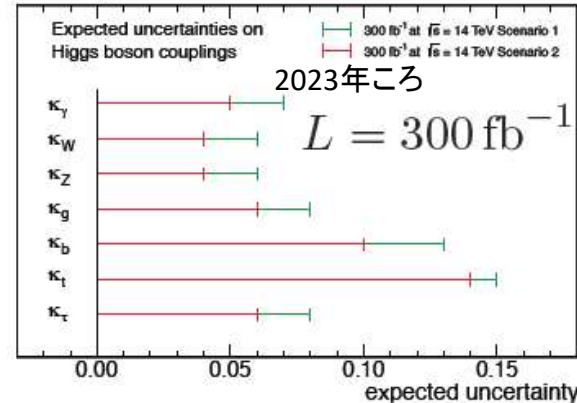
ATLAS Simulation Preliminary

$\sqrt{s} = 14 \text{ TeV}$: $\int L dt = 300 \text{ fb}^{-1}$; $\int L dt = 3000 \text{ fb}^{-1}$

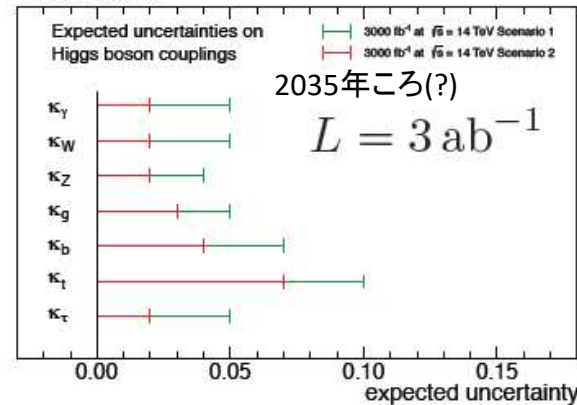


CMS Projection

CMS NOTE-13-002



CMS Projection



	$\sigma(14\text{TeV})/\sigma(8\text{TeV})$
$gg \rightarrow H$	2.6 ($M_X = M_H$)
$qq \rightarrow qqH$	2.6 (probes high M_X)
$qq \rightarrow VH$	2.1 ($M_X = M_V + M_H$)
$gg \rightarrow ttH$	4.7 (phase space + M_X)

CMS

Scenario 1

current systematic uncert.

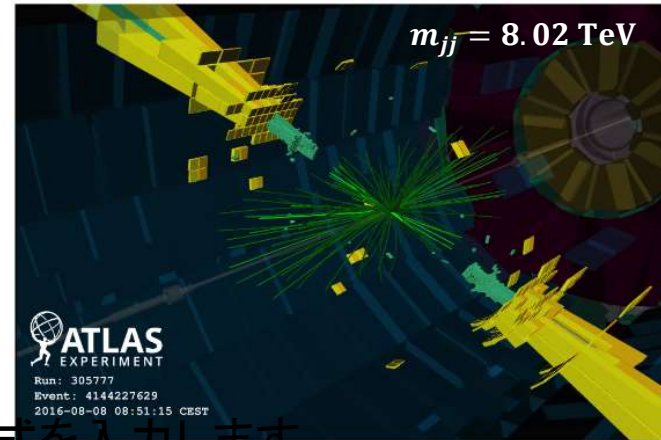
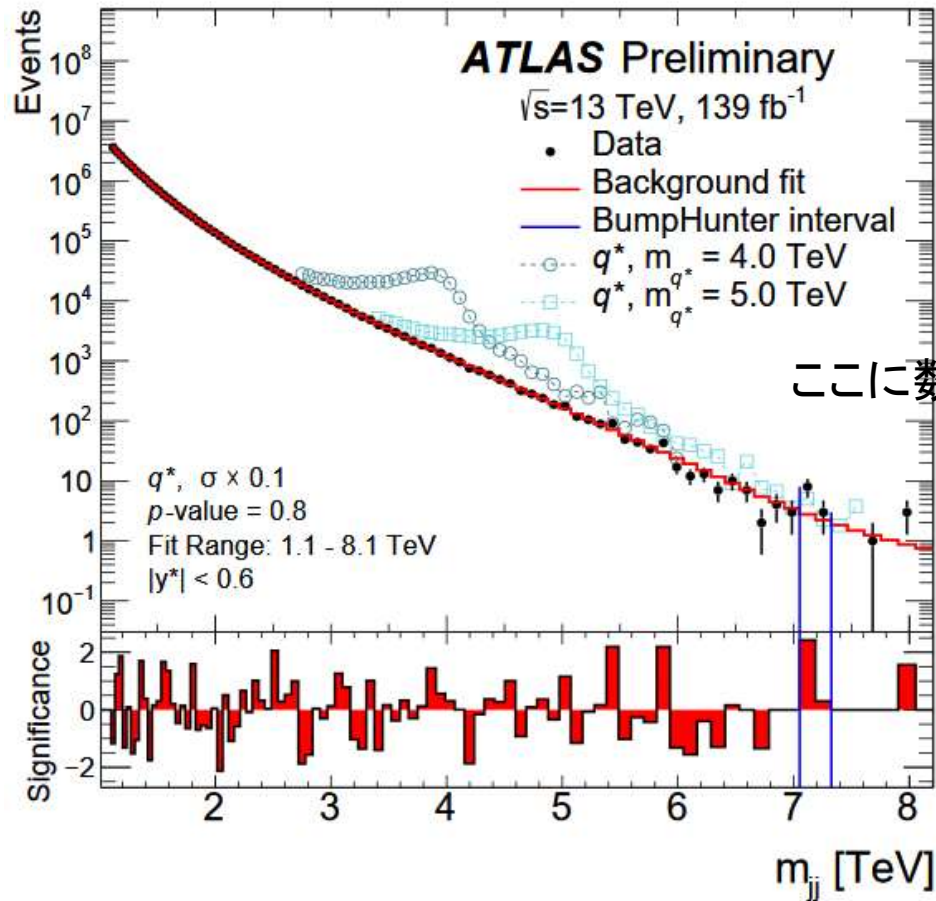
Scenario 2

theory uncert. $\searrow 1/2$

other systematics $\searrow 1/\sqrt{L}$

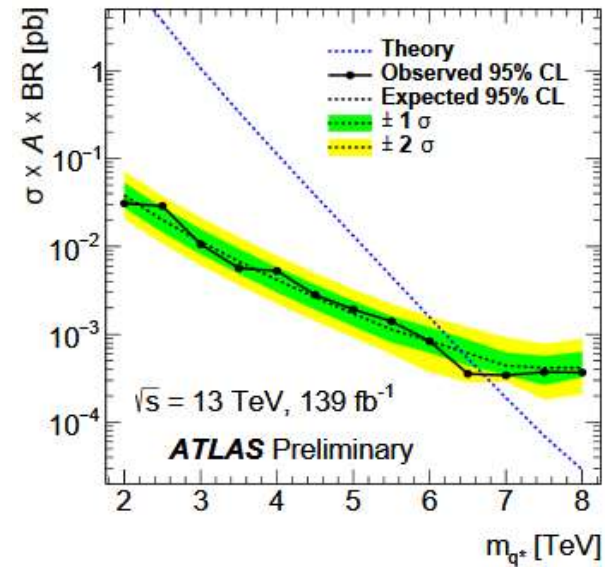
Full Run 2 Dijet Resonance Search

Dijet mass spectrum



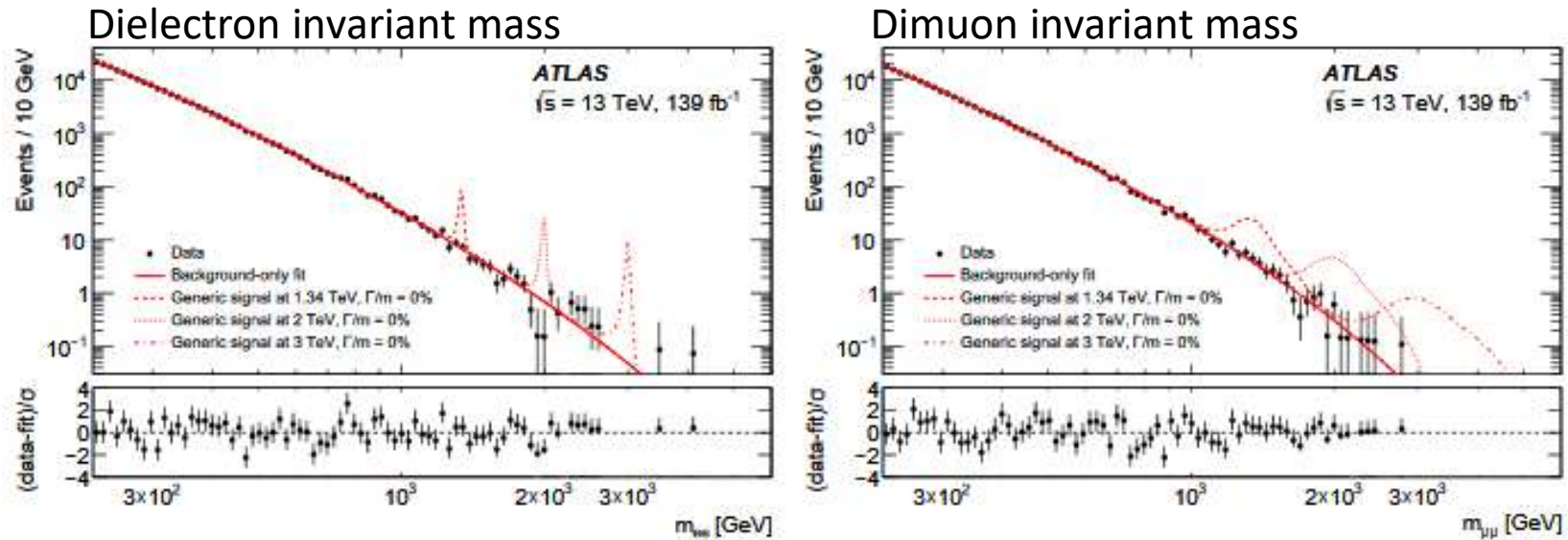
ここに数式を入力します。

Limit on excited quark model

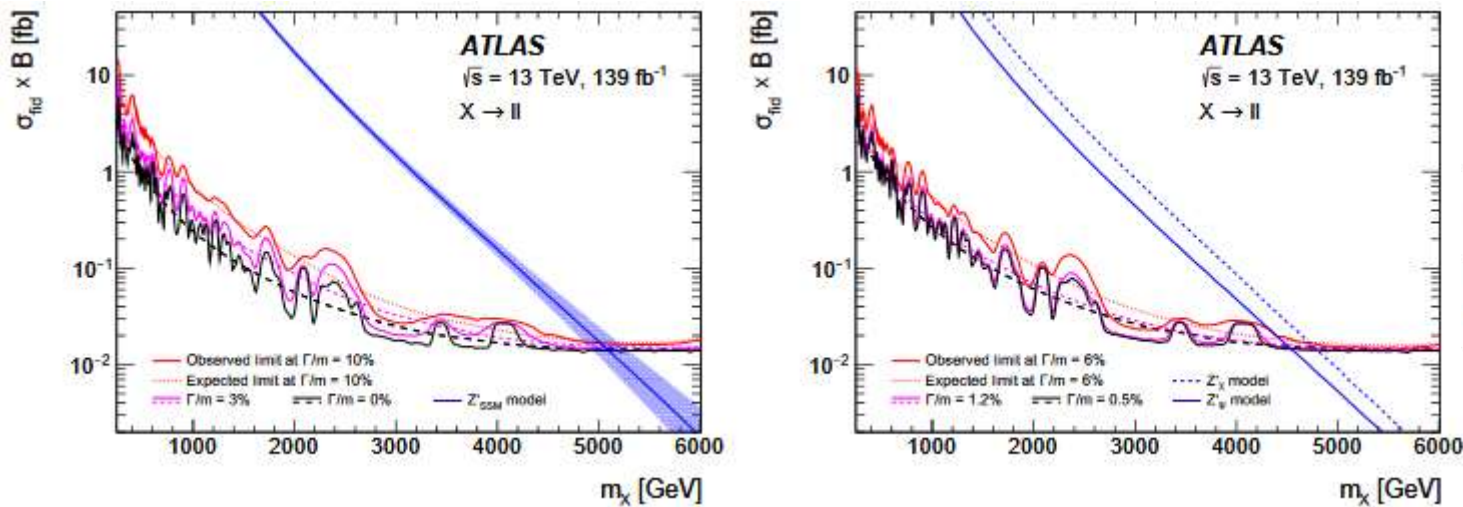


$$m_{q^*} > 6.7 \text{ TeV}$$

Full Run 2 Dilepton Resonance Search



No significant excess, set limit on production cross section of heavy particle.

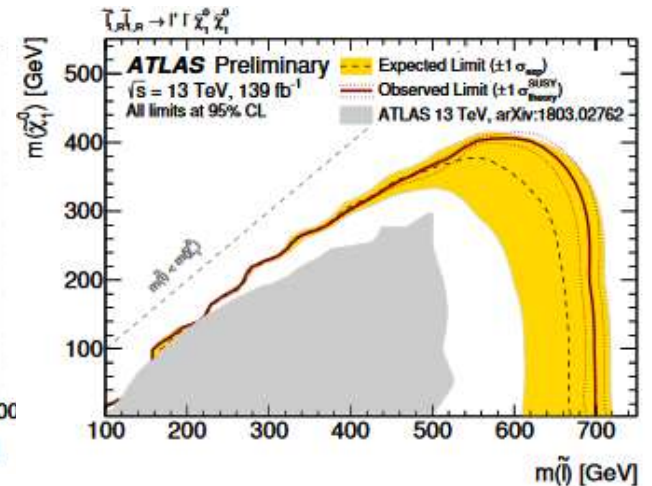
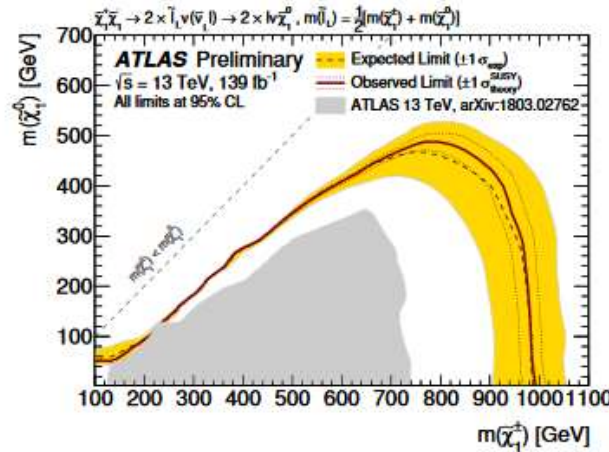
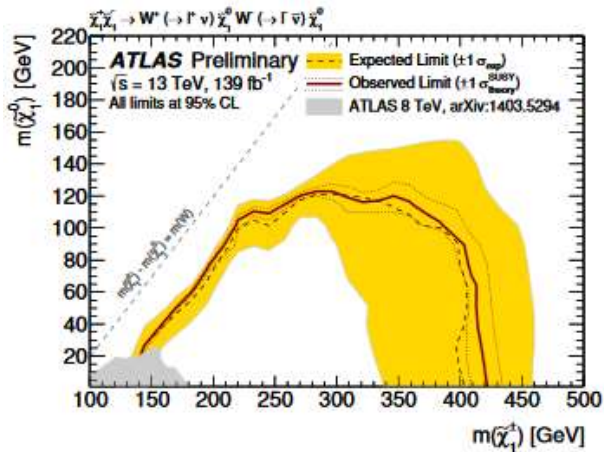
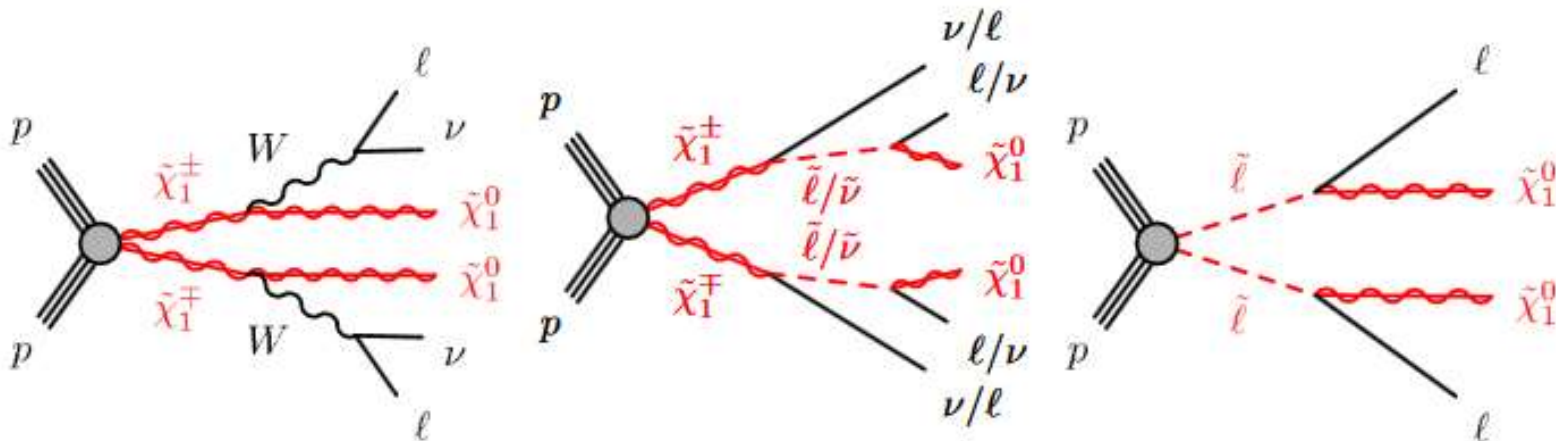


Lower limit on Z' mass

Model	Lower limits on $m_{Z'}$ [TeV]					
	ee		$\mu\mu$		$\ell\ell$	
	obs	exp	obs	exp	obs	exp
Z'_ψ	4.1	4.3	4.0	4.0	4.5	4.5
Z'_χ	4.6	4.6	4.2	4.2	4.8	4.8
Z'_{SSM}	4.9	4.9	4.5	4.5	5.1	5.1

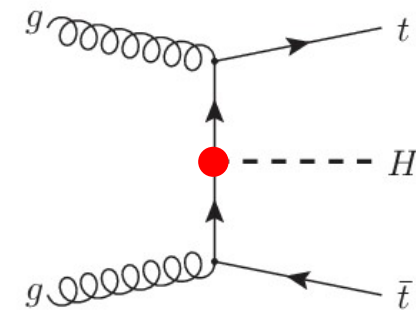
Chargino and Slepton Searches

- Final states: $2\ell + \text{missing } E_T$
- Use transverse mass M_{T2}



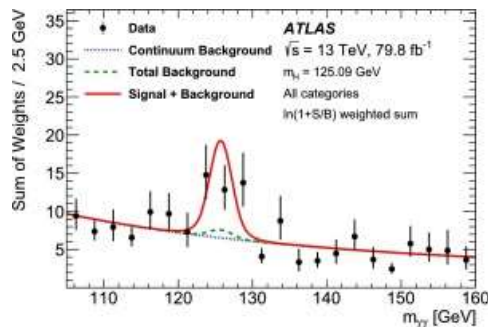
Observation of ttH production

- Top quarkの湯川カップリングを直接測定
- Combination of analyses with decays:
 - $H \rightarrow \gamma\gamma$ (79.8 fb^{-1})
 - $H \rightarrow WW/ZZ \rightarrow leptons$ (36.1 fb^{-1})
 - $H \rightarrow \bar{b}b$ (36.1 fb^{-1}) ← 本多D論(2018)

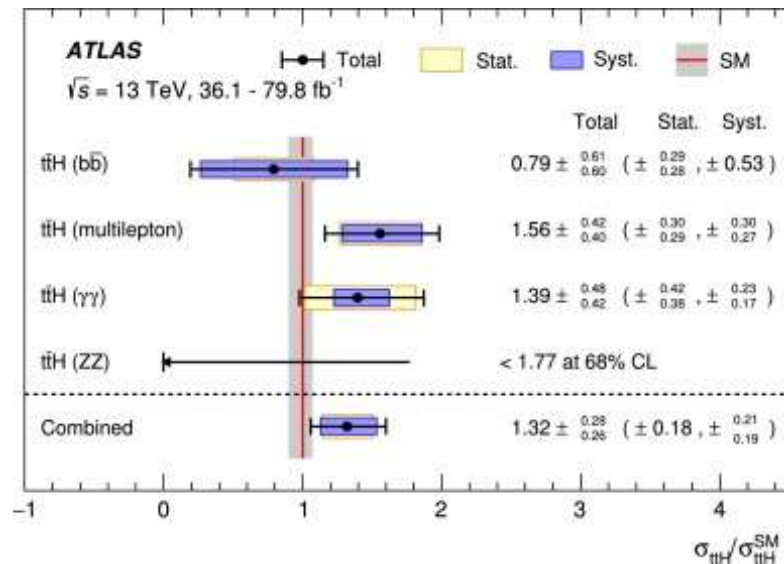
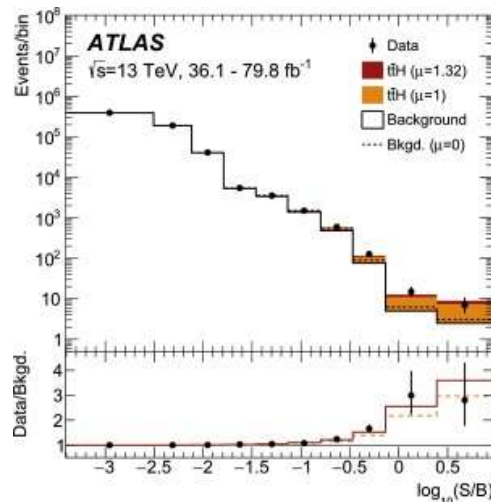


Candidate eventのS/B分布 測定された信号強度

$H \rightarrow \gamma\gamma$ イベント



単独だと、 3.7σ

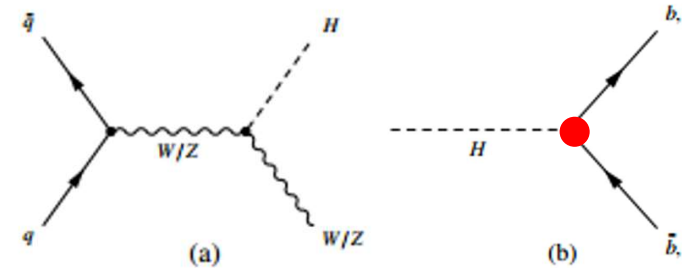


5.8σ Observation

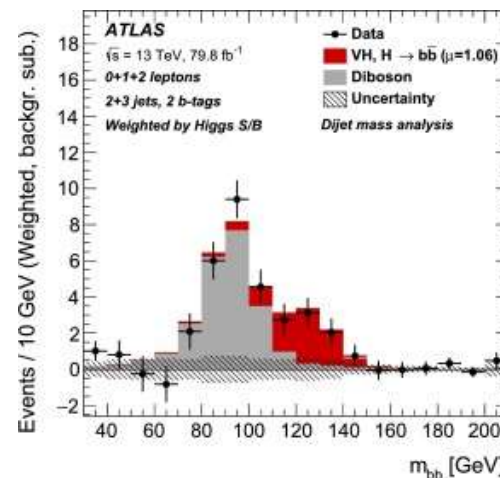
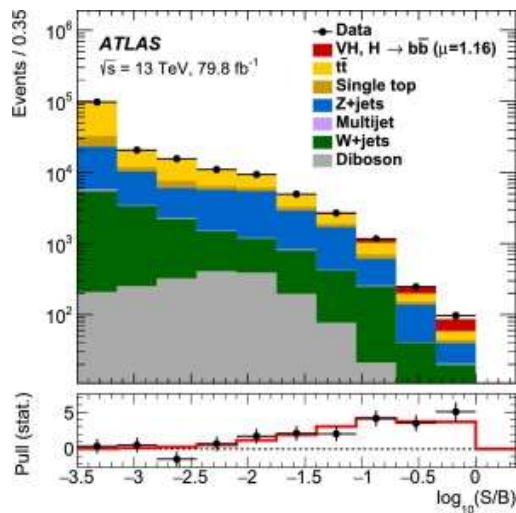
(expected sensitivity: 4.9σ)

Observation of $H \rightarrow b\bar{b}$

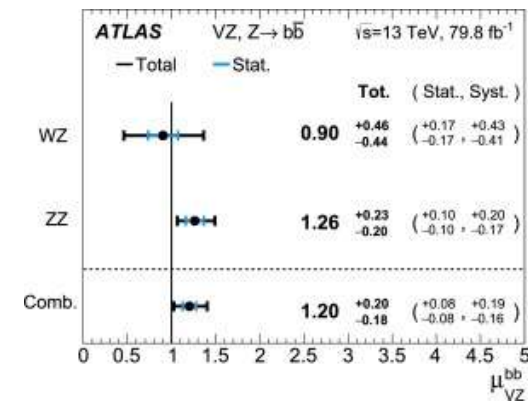
- bottom quarkの湯川カップリング
- Combination of processes:
 - $ZH \rightarrow (\nu\nu)(bb)$
 - $WH \rightarrow (\ell\nu)(bb)$
 - $ZH \rightarrow (\ell\ell)(bb)$



Candidate eventのS/B分布 m_{bb} 分布



測定された信号強度



5.3 σ Observation
 (expected sensitivity: 4.8 σ) 38

HNL production and decay

$$\sigma(pp \rightarrow W) \cdot \mathcal{B}(W \rightarrow \ell N) = \sigma(pp \rightarrow W) \cdot \mathcal{B}(W \rightarrow \ell \nu) \cdot |U|^2 \left(1 - \frac{m_N^2}{m_W^2}\right)^2 \left(1 + \frac{m_N^2}{2m_W^2}\right). \quad (1)$$

2.2 HNL decay

For this search, partial widths are calculated for all HNL decay channels including leptons and quarks. The calculations consider charged- and neutral-current-mediated interactions as well as QCD loop corrections, which are all described in Ref. [26]. The HNL lifetime τ_N has a strong dependence on the coupling strength $|U|^2$ and also the mass m_N due to phase-space effects. For a given $|U|^2$ and m_N , the total width $\Gamma = \sum_i \Gamma_i(m_N, |U|^2)$ is computed, and the mean lifetime is obtained as $\tau_N = \hbar/\Gamma$. In the relevant range $4.5 \leq m_N \leq 50$ GeV, the result agrees within 2% with the following parameterisations given in Ref. [27]: $\tau_{N_\mu} = (4.49 \cdot 10^{-12} \text{ s})|U|^{-2}(m_N/1 \text{ GeV})^{-5.19}$ and $\tau_{N_e} = (4.15 \cdot 10^{-12} \text{ s})|U|^{-2}(m_N/1 \text{ GeV})^{-5.17}$ for dominant mixing to ν_μ and ν_e , respectively. These relationships, however, assume no LNV decays. If LNV is allowed, twice as many decay channels are allowed, and τ_N is reduced by a factor of 2. More elaborate models do not necessarily allow for LNV [23] and thus may or may not contain this factor of 2. To account for this model dependence, both interpretations are considered in the case of the displaced signature, which is not limited to LNV processes.